

A BROAD BAND BI-DIRECTIONAL COUPLER
WITH TIGHT COUPLING AND
HIGH DIRECTIVITY.

ROBERT ANSEL EIDSON

1953

Library
U. S. Naval Postgraduate School
Monterey, California

17-86

**A BROAD BAND BI-DIRECTIONAL
COUPLER WITH TIGHT COUPLING
AND HIGH DIRECTIVITY**

R. A. Eidson

7-11-11 11-11 11-11 11-11

11-11 11-11 11-11 11-11

11-11 11-11 11-11 11-11

11-11 11-11 11-11 11-11

A BROAD BAND BI-DIRECTIONAL
COUPLER WITH TIGHT COUPLING
AND HIGH DIRECTIVITY

by

Robert Ansel Eidson,
Lieutenant, United States Navy

Submitted in partial fulfillment
of the requirements
for the degree of

MASTER OF SCIENCE

United States Naval Postgraduate School
Monterey, California
1953

E29

THE UNIVERSITY OF CHICAGO
LIBRARY
530 EAST 5TH STREET
CHICAGO, ILL. 60607

20

THE UNIVERSITY OF CHICAGO
LIBRARY

THE UNIVERSITY OF CHICAGO
LIBRARY
530 EAST 5TH STREET
CHICAGO, ILL. 60607

CHICAGO, ILL. 60607

THE UNIVERSITY OF CHICAGO
LIBRARY
530 EAST 5TH STREET
CHICAGO, ILL. 60607

This work is accepted as fulfilling
the thesis requirements for the degree of

MASTER OF SCIENCE

IN

ENGINEERING ELECTRONICS

from the

United States Naval Postgraduate School.

PREFACE

A directional coupler is an electromagnetic device by which the magnitude of the voltage incident on and reflected by a load can be monitored. Since broad band operation is becoming a requirement for most microwave systems, the power measuring device must also become broad band. This paper deals with the design and development considerations of such a broad band bi-directional coupler.

This work is an outgrowth of a need for such a coupler in a Swept Frequency Oscillator System currently under development at Dalmo-Victor Company, San Carlos, California. The actual bi-directional coupler developed at Dalmo-Victor from the theory to be presented here, substantiates this method as a practical means of broad band directional coupler design.

The theory employed is not original. It is primarily the result of correlating and applying the work of several outstanding men in the electromagnetic field. Their contributions are noted throughout the body of this paper.

My sincere thanks to Professors C. E. Menneken and W. M. Bauer who as first and second readers contributed materially to this thesis by their helpful suggestions and criticisms.

R. A. Eidson

A directional coupler is an electronic device which is used to measure the magnitude of the voltage level of an antenna or a line. Since such a device can be monitored, it is useful for most electronic systems, and it is a very important part of many electronic systems. This paper describes the design and development considerations of a directional coupler.

This work is an outgrowth of a more general study in the design of a directional coupler. The design of a directional coupler is a complex task, and it is not possible to design a directional coupler without a detailed knowledge of the theory of directional couplers. The theory of directional couplers is presented here, and it is shown that the theory of directional couplers is not original. It is shown that the theory of directional couplers is a special case of the theory of directional couplers. The theory of directional couplers is presented here, and it is shown that the theory of directional couplers is a special case of the theory of directional couplers. The theory of directional couplers is presented here, and it is shown that the theory of directional couplers is a special case of the theory of directional couplers.

The theory of directional couplers is presented here, and it is shown that the theory of directional couplers is a special case of the theory of directional couplers. The theory of directional couplers is presented here, and it is shown that the theory of directional couplers is a special case of the theory of directional couplers. The theory of directional couplers is presented here, and it is shown that the theory of directional couplers is a special case of the theory of directional couplers.

TABLE OF CONTENTS

	Page
CERTIFICATE OF APPROVAL	i
PREFACE	ii
LIST OF ILLUSTRATIONS	iv
TABLE OF SYMBOLS AND ABBREVIATIONS	v
CHAPTER	
I. INTRODUCTION	1
1. Summary	
2. Definitions	
3. Possible Uses	
4. Comparison with Slotted Lines and Hybrids	
II. DESIGN CONSIDERATIONS	8
1. General	
2. Coupling	
3. Directivity	
III. THEORETICAL DESIGN	16
IV. EXPERIMENTAL RESULTS	26
V. CONCLUSION	29
1. General	
2. Coupling	
3. Directivity	
BIBLIOGRAPHY	33
APPENDIX A	34
APPENDIX B	37

1	CONTENTS
1	PREFACE
1	LIST OF ABBREVIATIONS
1	TABLE OF SYMBOLS
1	CHAPTER I
1	1. INTRODUCTION
	1.1. General
	1.2. Definitions
	1.3. Formalism
	1.4. Consequences
	1.5. Summary
1	2. CONCLUSION
	2.1. General
	2.2. Conclusions
	2.3. Summary
1	3. REFERENCES
1	4. APPENDICES
	4.1. Appendix A
	4.2. Appendix B
	4.3. Appendix C
	4.4. Appendix D
	4.5. Appendix E
	4.6. Appendix F
	4.7. Appendix G
	4.8. Appendix H
	4.9. Appendix I
	4.10. Appendix J
	4.11. Appendix K
	4.12. Appendix L
	4.13. Appendix M
	4.14. Appendix N
	4.15. Appendix O
	4.16. Appendix P
	4.17. Appendix Q
	4.18. Appendix R
	4.19. Appendix S
	4.20. Appendix T
	4.21. Appendix U
	4.22. Appendix V
	4.23. Appendix W
	4.24. Appendix X
	4.25. Appendix Y
	4.26. Appendix Z

LIST OF ILLUSTRATIONS

	Page
1. Block diagram of Swept Frequency Oscillator System	-2a-
2. Directional coupler definitions	-2b-
3. Directivity of a bi-directional coupler	-9a-
4. Coupling element taper	-11a-
5. Constant coupling plate by Miller-Mumford	-13a-
6. Tapered coupling plate by Miller-Mumford	-13a-
7. Superimposition of Tchebyscheff coefficients by Barnett	-19a-
8. Final Design of coupling plate	-19b-
9. Wave guide dimensions	-20a-
10. $F_A(\lambda_g)$ versus x_1	-22a-
11. $F_A(\lambda_g)$ versus λ_g	-23a-
12. Photograph of directional coupler	-26b-
13. Test bench set-up	-26a-
14. Theoretical and actual coupling curves	-26c-
15. The technique used for measuring directivity	-26d-
16. Theoretical and actual directivity curves.	-28a-

TABLE OF SYMBOLS AND ABBREVIATIONS

a	Large internal rectangular wave guide dimension.
A_n	Voltage coupling coefficient in the forward wave direction for the n^{th} hole.
A_T	Total voltage coupling coefficients for all n longitudinally distinct holes.
b	small internal rectangular wave guide dimension.
B_n	Voltage coupling coefficient in the backward wave direction for the n^{th} hole.
C	Coupling in decibels.
D	Directivity in decibels.
d_n	Diameter of the n^{th} longitudinally distinct coupling hole.
n	An integer from 1 to n , numbering the longitudinally distinct coupling holes.
$2N$	Total number of longitudinally distinct coupling holes.
r_n	Radius of the n^{th} longitudinally distinct coupling hole.
t	Thickness of the common plate between the main and auxiliary wave guide.
T_n	Tchebyscheff coefficient for the n^{th} longitudinally distinct coupling hole.
T_T	Total of Tchebyscheff coefficients of all n coupling holes.
VSWR	Voltage Standing Wave Ratio.
x, y, z	Large dimension (a) axis, small dimension (b) axis, and longitudinal axis of the wave guide, respectively.
x_1	Dimension in the direction of the x -axis from the internal side wall to the center of a coupling hole. A constant for all n holes.

1	Introduction	1
2	Objectives of the Study	2
3	Methodology	3
4	Results and Discussion	4
5	Conclusion	5
6	References	6
7	Appendix	7
8	Bibliography	8
9	Index	9
10	Summary	10
11	Abstract	11
12	Keywords	12
13	Notes	13
14	Footnotes	14
15	Endnotes	15
16	References	16
17	Appendix	17
18	Bibliography	18
19	Index	19
20	Summary	20
21	Abstract	21
22	Keywords	22
23	Notes	23
24	Footnotes	24
25	Endnotes	25
26	References	26
27	Appendix	27
28	Bibliography	28
29	Index	29
30	Summary	30
31	Abstract	31
32	Keywords	32
33	Notes	33
34	Footnotes	34
35	Endnotes	35
36	References	36
37	Appendix	37
38	Bibliography	38
39	Index	39
40	Summary	40
41	Abstract	41
42	Keywords	42
43	Notes	43
44	Footnotes	44
45	Endnotes	45
46	References	46
47	Appendix	47
48	Bibliography	48
49	Index	49
50	Summary	50
51	Abstract	51
52	Keywords	52
53	Notes	53
54	Footnotes	54
55	Endnotes	55
56	References	56
57	Appendix	57
58	Bibliography	58
59	Index	59
60	Summary	60
61	Abstract	61
62	Keywords	62
63	Notes	63
64	Footnotes	64
65	Endnotes	65
66	References	66
67	Appendix	67
68	Bibliography	68
69	Index	69
70	Summary	70
71	Abstract	71
72	Keywords	72
73	Notes	73
74	Footnotes	74
75	Endnotes	75
76	References	76
77	Appendix	77
78	Bibliography	78
79	Index	79
80	Summary	80
81	Abstract	81
82	Keywords	82
83	Notes	83
84	Footnotes	84
85	Endnotes	85
86	References	86
87	Appendix	87
88	Bibliography	88
89	Index	89
90	Summary	90
91	Abstract	91
92	Keywords	92
93	Notes	93
94	Footnotes	94
95	Endnotes	95
96	References	96
97	Appendix	97
98	Bibliography	98
99	Index	99
100	Summary	100

- z_0 A design parameter which determines the width of the suppression band of a Tchebyscheff array.
- Z_0 Characteristic impedance.
- z_1 Dimension in the direction of the z-axis from the center of one coupling hole to the center of the next. A constant for all n holes.
- α_E Attenuation coefficient for the E-field which compensates for the finite "t" in a wave guide coupler.
- α_H Attenuation coefficient for the H-field which compensates for the finite "t" in a wave guide coupler.
- β Wave number equal to $2\pi/\lambda_g$
- Γ Voltage coefficient of reflection.
- λ_g Guide Wave-length
- λ_0 Free space wave-length
- ρ Geometric factor depending on the radius of a coupling hole and the thickness, t.

1. Description of the system and its components	1
2. Theoretical background and assumptions	2
3. Experimental setup and procedure	3
4. Results and discussion	4
5. Conclusions	5
6. Acknowledgments	6
7. References	7
8. Appendix A: Mathematical derivations	8
9. Appendix B: Experimental data	9
10. Appendix C: Glossary of terms	10
11. Appendix D: List of symbols	11
12. Appendix E: Bibliography	12

CHAPTER I

INTRODUCTION

1. Summary

Assuming that oscillators are available which will tune across the frequency band of a particular standard guide, the antenna load matching problem still confronts the radar engineer. Supposedly, broad band antennas have been designed. This should mean that there are no frequencies within the design bandwidth of the antenna at which high reflections occur. However, such antennas can only be tested at a finite number of selected frequencies unless a swept frequency oscillator system is used. The desired frequency bandwidth must be swept at a speed slow enough to give good resolution. This sweep is placed on the horizontal plates of an indicator. The swept frequency output is attached to a bi-directional coupler, whose main guide output goes to the antenna load. The two coupler outputs from the auxiliary guide proportional to the incident and reflected voltage of the load, are amplified through two separate logarithmic amplifiers. The logarithmic outputs go next to a difference amplifier from which the quotient of the reflected voltage to the incident voltage (coefficient of reflection) can be obtained. This quotient is related to the voltage standing wave ratio by the following well know formula:

$$VSWR = \frac{1 + |\Gamma|}{1 - |\Gamma|} \quad \text{where } |\Gamma| = \left| \frac{E_{ref}}{E_{inc}} \right| \quad (1)$$

This quotient signal is placed on the vertical plates on the indicator whose face is calibrated with known values of VSWR. A block diagram of this system is illustrated in figure (1).

By use of this system, it is readily ascertained if there are any frequencies where a bad mismatch of antenna to transmission wave guide exist. The accuracy of the entire system depends upon the accuracy with which the two coupler output voltages can be obtained. The bi-directional coupler separates these two voltages and must therefore be carefully designed.

2. Definitions

Practically every term of the directional coupler theory is defined differently, depending upon the author. An attempt will be made (1) to define only those terms used in this paper, (2) to use the most common, and if possible, logical definitions, and (3) to adhere consistently to these definitions throughout the text.

Directional couplers are used in both coaxial and wave guide systems. Only wave guide directional couplers will be considered in this paper.

A directional coupler is a means of coupling electromagnetic waves from a main transmission guide to an auxiliary guide. It has the property of propagating the wave which is traveling in the auxiliary guide in the direction of the main guide wave (forward wave), while attenuating the wave in the auxiliary guide which is traveling in the direction opposite to the main guide wave (backward wave). See figure (2).

and went straight to the telephone and called the police.

000000000000

...the ...
...the ...
...the ...
...the ...
...the ...
...the ...
...the ...

in the direction of the main axis of the body, and the direction of the main axis of the body is the direction of the main axis of the body.

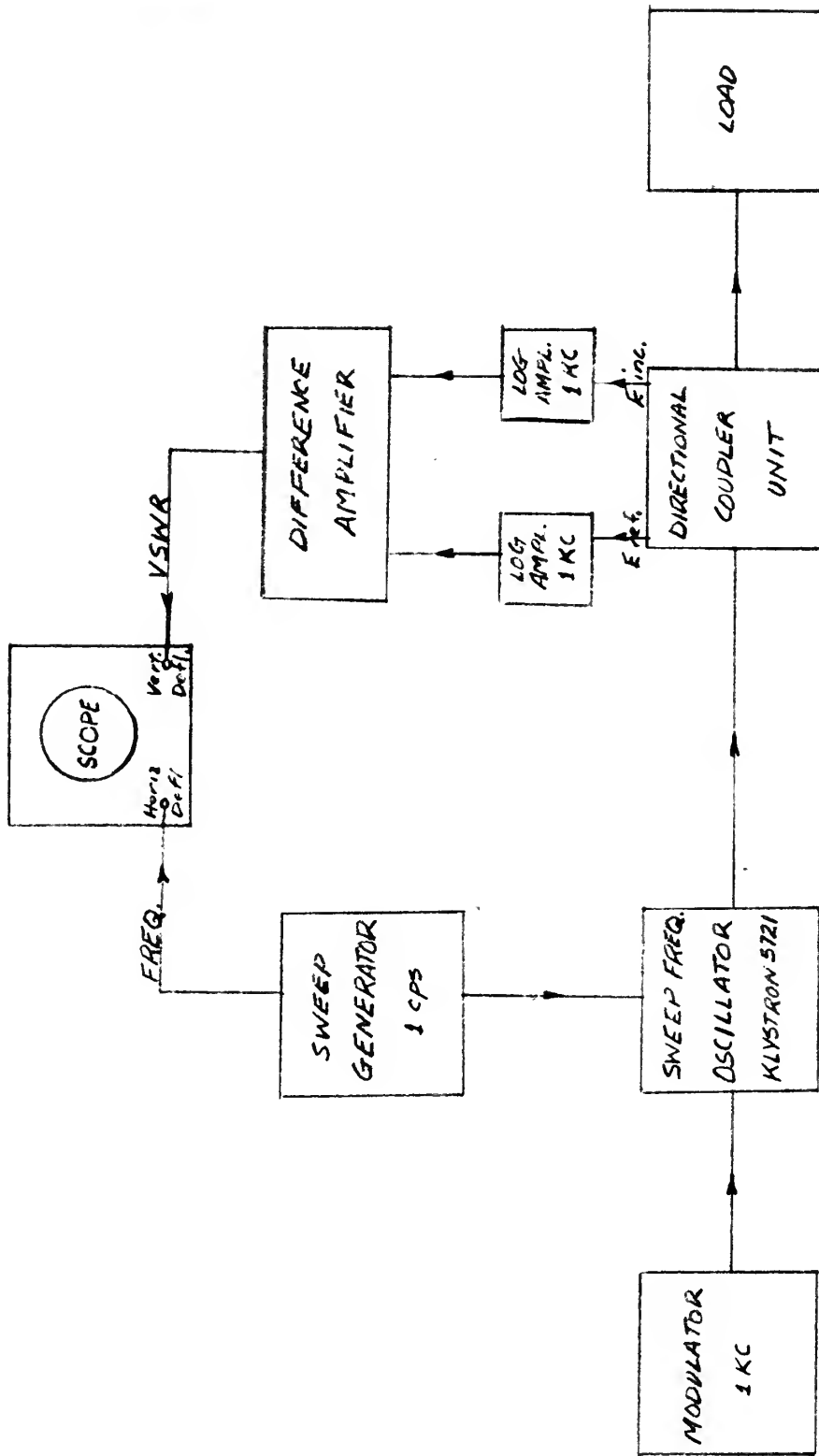
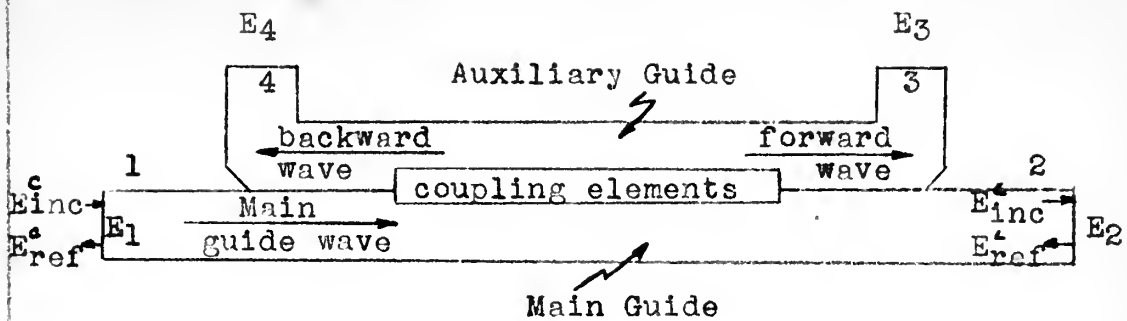


FIGURE (1)



E_1, E_2, E_3, E_4 - voltages across terminals 1, 2, 3, 4.

$$(1) \text{ Coupling*in db} = C = 20 \log \frac{|E_3|}{|E_1|}$$

$$(2) \text{ Directivity*in db} = D = 20 \log \frac{|E_3|}{|E_4|}$$

$$(3) |VSWR_{\text{coupler}}| = \frac{|E_{\text{inc}}^c| + |E_{\text{ref}}^c|}{|E_{\text{inc}}^c| - |E_{\text{ref}}^c|}$$

$$|VSWR_{\text{load}}| = \frac{|E_{\text{inc}}^L| + |E_{\text{ref}}^L|}{|E_{\text{inc}}^L| - |E_{\text{ref}}^L|} = \frac{|E_3| + |E_4|}{|E_3| - |E_4|}$$

$$(4) |\Gamma_L| = \frac{|E_{\text{ref}}^L|}{|E_{\text{inc}}^L|} = \frac{|E_4|}{|E_3|}$$

* For measurement of these, all terminals must be perfectly matched.

DIRECTIONAL COUPLER DEFINITIONS

FIGURE (2)

It should be noted that directional couplers are symmetrical, which means they may be turned end for end with no effect on their external behavior. Referring to figure (2), it is seen that a voltage fed in at terminal 1 will divide between terminals 2 and 3, without appearing at terminal 4; while a voltage fed in at terminal 2 will divide between terminals 1 and 4 without appearing at terminal 3. In order for this statement to be strictly valid, the ideal conditions of perfectly matched terminations and perfect directivity must exist. However, this does serve to illustrate the principal properties of coupling and directivity of a directional coupler.

The auxiliary guide of the coupler usually has a single output with the other end terminated in its characteristic impedance, Z_0 . The coupler therefore is capable of monitoring only the incident or the reflected wave at one time, depending upon its orientation in the wave guide system. It is of course possible to place two such couplers back to back* to monitor the incident and reflected wave at the same time. This gives isolation to each auxiliary output arm but doubles the length of the overall coupling system.

A bi-directional coupler has two outputs in the auxiliary guide. It has the advantages over the single-ended back to back coupling of being shorter and using common coupling elements for both outputs.

*When two single output directional couplers have their main guide connected in the wave guide system, with the coupler closest to the source positioned to monitor the incident voltage and the coupler closest to the load positioned to monitor the reflected voltage, they are said to be back to back.

It should be noted that these two couplers are identical, which means they may be turned end for end with no effect on the external behavior. Referring to Figure 2, it is seen that the voltage fed in at terminal 1 will divide between terminals 2 and 3, without appearing at terminal 4; while a voltage fed in at terminal 2 will divide between terminals 1 and 3 without appearing at terminal 4. In order for this statement to be valid, the ideal conditions of perfectly matched terminations at terminals 1 and 2 must exist. However, this does not hold for a general principle properties of coupling and directivity of a directional coupler.

The auxiliary guide of the coupler usually has a length equal to that of the other and terminated in its characteristic impedance. The coupler therefore is capable of monitoring only the incident or the reflected wave in one line, depending upon its termination in the wave guide system. It is of course possible to place the couplers back to back, so that for the incident and reflected waves the same time. This gives isolation to each direction of travel, but doubles the length of the overall coupling device.

A bi-directional coupler has two outputs to the main line. It has the advantages over the single-ended type that it is capable of being inserted and being removed conveniently without the need of being reconnected to the main line. When two single output directional couplers are connected in series, as shown in Figure 3, the output voltage at each source positioned to monitor the incident voltage will be identical to the total voltage at the input. They are said to be back to back.

However, these two arms have no isolation between them, which means that any reflection due to detector mismatch will introduce an error.

Coupling elements are the physical means of coupling power from the main to the auxiliary guide. They take the form of probes, loops, or apertures of any shape and size placed anywhere in either the large or small faces of the guide.

Coupling is one of two main terms which serve to specify the performance of a coupler. It is simply an indication of the amount of voltage coupled from the main to the auxiliary guide, as shown in figure (2), equation (1). Coupling is most commonly expressed in decibels as the ratio of the voltage delivered to the forward arm of the auxiliary guide to the voltage input to the coupler. Therefore, the coupling as defined here will always appear as a negative number of db. If a coupler is said to have -10db coupling, or just 10 db coupling, this means the voltage delivered to the forward arm of the auxiliary guide is 10 db below the input voltage.

Directivity is the second term which specifies the performance of a coupler. It represents the effectiveness with which a coupler attenuates a backward wave and propagates the forward wave in the auxiliary guide. It is most commonly given in db and is the ratio of the voltage of the forward wave to the voltage of the backward wave in the auxiliary guide. A coupler with 20 db directivity contains voltage in the backward wave which is 20 db below the voltage in the forward wave.

The VSWR of a coupler is often specified. However, when using Bethe's small hole theory for coupler design, the reflections of the coupler are usually so small compared with other reflections that they are insignificant.

large in a well known of the old

The following information was obtained from the records of the [redacted] Department.

[Redacted]

1. The first of these is the fact that the United States is a democratic country.

Reflection Coefficient, $|\Gamma|$, is the ratio of the reflected voltage to the incident voltage.

Each of these last four terms are illustrated in figure (2) for a bi-directional coupler.

All future references to "couplers" will apply to directional couplers unless otherwise specified.

3. Possible Uses

Directional couplers have many uses in wave guide systems. Of these uses, the two most important are its use in monitoring a source, and its use in monitoring a load.

In monitoring a source, a coupler may monitor the power, the frequency, or the frequency spectrum of a transmitted pulse. As a power monitor, the coupler will also be an attenuator, the amount of attenuation required depending upon the sensitivity of the detection unit. With the attenuation a desirable feature, this type coupler will have loose coupling usually -20 db or less. The directivity of this coupler need not be high since for a fixed load and frequency, any error introduced in source power measurements by low directivity may be calibrated out.

In monitoring a load, a coupler will give an indication of how well the load is matched to the source. The coupling required for this coupler is a function of the sensitivity desired at the detector output. However, high directivity is required to measure small reflections. With a perfectly matched load (VSWR equal one), there would be no reflected voltage; therefore, the output voltage E_4 of

1. The first step in the process of identifying a problem is to define the problem. This involves identifying the symptoms of the problem and determining the scope of the problem. Once the problem has been defined, the next step is to identify the causes of the problem. This involves identifying the factors that are contributing to the problem and determining the relationships between these factors. Once the causes of the problem have been identified, the next step is to develop a plan of action. This involves identifying the steps that need to be taken to solve the problem and determining the resources that will be needed to implement the plan. Once a plan of action has been developed, the next step is to implement the plan. This involves carrying out the steps that have been identified in the plan and monitoring the progress of the implementation. Finally, the last step in the process is to evaluate the results of the implementation. This involves determining whether the problem has been solved and whether the resources have been used effectively.

figure (2) should be zero since E_4 is proportional to E_{ref} . If E_4 is zero, then from equation (2) of figure (2), the directivity, D , is equal to infinity. This is perfect directivity and it means that none of the voltage of the main guide wave incident at terminal 1 travels in the backward direction in the auxiliary guide. With finite hole sizes for coupling elements, this is impossible even at a single frequency. However, directivities high enough to measure practical load VSWRs can be attained. For example, if it is desirable to measure the VSWR of a load down to 1.05, the directivity must be high enough not to introduce error signals which would be of the same order of magnitude as the reflection to be measured. A directivity of 32.2 db would introduce an error of equal magnitude as the reflection of a 1.05 load. If an attempt were made to measure a 1.05 load with a coupler having only 32.2 db directivity, by mechanically positioning the load, the magnitude of the voltage across the backward arm, E_4 , would range from zero to twice the correct voltage. This variation is the result of the phase difference between the two equal magnitude voltages concerned. Therefore, in order to reduce the directivity error voltage to one-fifth of the reflected voltage of a 1.05 load, a directivity of 46 db is required.

If a single-ended directional coupler is set up to monitor reflected voltages, the reflected indication can be used to tune the load to a minimum reflection. However, if it is desired to read the coefficient of reflection without reversing the coupler, a bi-directional coupler must be used. This is the usage which fostered this study and the design of the coupler described later.

1. The first part of the document is a letter from the President of the United States to the Congress, dated January 3, 1862. It is a very important document, as it contains the President's views on the state of the Union and the progress of the war. The President discusses the military situation, the financial state of the country, and the political climate. He also mentions the recent death of General Grant and the appointment of General Sherman to command the Army of the Potomac.

2. The second part of the document is a report from the Secretary of the Treasury, dated January 10, 1862. It provides a detailed account of the financial operations of the government during the year 1861. The report includes information on the revenue, the expenditures, and the public debt. It also discusses the various measures that have been taken to manage the finances of the government during the war.

3. The third part of the document is a report from the Secretary of the Interior, dated January 15, 1862. It provides a detailed account of the operations of the Department of the Interior during the year 1861. The report includes information on the land sales, the mineral resources, and the various bureaus and offices within the department. It also discusses the various measures that have been taken to manage the affairs of the department during the war.

4. The fourth part of the document is a report from the Secretary of the War, dated January 20, 1862. It provides a detailed account of the military operations of the government during the year 1861. The report includes information on the various campaigns, the battles, and the movements of the army. It also discusses the various measures that have been taken to manage the military affairs of the government during the war.

5. The fifth part of the document is a report from the Secretary of the Navy, dated January 25, 1862. It provides a detailed account of the operations of the Department of the Navy during the year 1861. The report includes information on the various ships, the crews, and the various operations of the navy. It also discusses the various measures that have been taken to manage the affairs of the department during the war.

6. The sixth part of the document is a report from the Secretary of the Army, dated February 1, 1862. It provides a detailed account of the operations of the Department of the Army during the year 1861. The report includes information on the various regiments, the battalions, and the various operations of the army. It also discusses the various measures that have been taken to manage the affairs of the department during the war.

7. The seventh part of the document is a report from the Secretary of the Marine Corps, dated February 5, 1862. It provides a detailed account of the operations of the Marine Corps during the year 1861. The report includes information on the various companies, the battalions, and the various operations of the Marine Corps. It also discusses the various measures that have been taken to manage the affairs of the department during the war.

8. The eighth part of the document is a report from the Secretary of the Coast and Geodetic Survey, dated February 10, 1862. It provides a detailed account of the operations of the Coast and Geodetic Survey during the year 1861. The report includes information on the various surveys, the maps, and the various operations of the survey. It also discusses the various measures that have been taken to manage the affairs of the department during the war.

9. The ninth part of the document is a report from the Secretary of the Smithsonian Institution, dated February 15, 1862. It provides a detailed account of the operations of the Smithsonian Institution during the year 1861. The report includes information on the various collections, the research, and the various operations of the institution. It also discusses the various measures that have been taken to manage the affairs of the institution during the war.

10. The tenth part of the document is a report from the Secretary of the National Academy of Sciences, dated February 20, 1862. It provides a detailed account of the operations of the National Academy of Sciences during the year 1861. The report includes information on the various members, the research, and the various operations of the academy. It also discusses the various measures that have been taken to manage the affairs of the academy during the war.

Directional couplers have also been used to introduce a signal to test receiver sensitivity. Also couplers have application as mixers.

4. Comparison with Slotted Lines and Hybrids

Load impedances can be measured either by measuring the reflection coefficient or the VSWR of a load. A bi-directional coupler measures direct, while a slotted line measures VSWR only after moving the output probe to two separate positions. The accuracies of the two are comparable. Good slotted lines have accuracies of 2%. This compares with a directivity of 40 db. Carefully designed couplers can do even better than this, but it seems the slotted line has reached its ultimate accuracy because of the discontinuity introduced by any probe. However, the slotted line can measure phase and magnitude while a coupler measures only magnitude.

When measuring low reflections, measuring with a coupler is more accurate than measuring VSWR by a slotted line. If higher reflections are to be measured, the use of a slotted line will give more accurate results.

A -3db coupler has the same division of power between main and auxiliary guides as a hybrid magic tee. Low reflections can be measured with the same accuracy with either the tee or the coupler, since each has approximately the same degree of isolation between arms. A small hole coupler, however, has the very distinct advantage of having a VSWR of 1.05 or less across the guide frequency band, whereas the tee is very frequency sensitive.

CHAPTER II

DESIGN CONSIDERATIONS

1. General

The specifications for a directional coupler of tight coupling and high directivity across a frequency band are difficult to meet. The tight coupling requires relatively large coupling apertures; but the larger the apertures the greater the interaction between coupling elements and the lower the directivity. Thus, these specifications are incompatible in this respect. However, both coupling and directivity increase with the number of coupling apertures, all other variables held fixed. It then becomes apparent that the best way to meet these specifications is (1) to use coupling apertures as large as possible without interfering with directivity, and then (2) to use as many coupling apertures as necessary to meet the required coupling and directivity. This approach will make the length of the coupler a minimum for any given specifications.

Although there are other designs* which can be used to obtain tight coupling, the so called multi-path directional couplers furnish the best possibility of satisfying both tight coupling and high directivity. In this type coupler there are several coupling elements along the guide length; and, therefore, there are many paths for the waves to travel. The directivity and coupling are achieved by wave interference, constructive for the forward wave and destructive for the

* For example, near-resonant slot couplers and branch guide couplers.

J. G. S. 1907

For example, when a ship is moving through the water, the water molecules are displaced in a direction perpendicular to the direction of the ship's motion. This is because the water molecules are being pushed back and forth by the ship's hull, and this creates a transverse wave. The water molecules are not moving in the same direction as the ship, but rather in a direction perpendicular to the ship's motion. This is why the water molecules are displaced in a direction perpendicular to the direction of the ship's motion.

backward wave. The destructive interference is caused by phase difference due to path differences.

These multipath couplers are readily compared with antenna arrays. The voltage coefficient of directional couplers is computed in the same manner as the current feed of antenna arrays. Reference will be made to this comparison later.

First let us consider a two element coupler, which is the simplest form of multipath coupler. Its directivity is a result of (1) the quarter guide wave length spacing ($\lambda_g/4$) of coupling elements, and (2) the inherent directivity of a single hole as explained by Bethe.¹ The first of these is the greatest source of directivity and can be most easily explained by reference to figure (3). A voltage wave is transferred from the main to the auxiliary guide by each coupling element, which can be considered as a secondary source. Waves are emitted in all directions but wave motion is supported only along the guide in the TE_{10} mode. This means that each coupling element source transmits voltage waves in two directions. E_{B1} of figure (3) represents the voltage of the backward traveling wave (moving to the left) coupled through coupling element 1. E_{F1} represents the voltage of the forward traveling wave (moving to the right) coupled through coupling element 2. E_{F1} and E_{F2} travel the same path length and will reinforce to give a signal output at terminal 3 equal to E_{F1} plus E_{F2} . E_{B2} will be in phase opposition to E_{B1} since it has traveled one-half guide wave length further than E_{B1} . Therefore, the output at terminal 4 will be proportional to the difference of

backward wave. The effective distance of the interaction is a function of the distance of the input and output ports.

The voltage developed in the interaction region is proportional to the distance of the interaction region. The voltage developed in the interaction region is proportional to the distance of the interaction region.

Reference will be made to this configuration later.

First let us consider a two element coupling element. The distance of the interaction region is a function of the distance of the interaction region.

of (1) the distance of the interaction region is a function of the distance of the interaction region. (2) the distance of the interaction region is a function of the distance of the interaction region.

elements, and (3) the distance of the interaction region is a function of the distance of the interaction region.

by Bethe. The first of these is the distance of the interaction region. The distance of the interaction region is a function of the distance of the interaction region.

and can be used to calculate the distance of the interaction region. The distance of the interaction region is a function of the distance of the interaction region.

the wave in the interaction region. The distance of the interaction region is a function of the distance of the interaction region.

each coupling element, which can be considered as a two element coupling element. The distance of the interaction region is a function of the distance of the interaction region.

Waves are excited in all directions. The distance of the interaction region is a function of the distance of the interaction region.

along the guide in the z direction. The distance of the interaction region is a function of the distance of the interaction region.

element source transmits voltage waves in the z direction. The distance of the interaction region is a function of the distance of the interaction region.

(2) represents the voltage of the backward wave. The distance of the interaction region is a function of the distance of the interaction region.

the left) coupled through coupling element 1. The distance of the interaction region is a function of the distance of the interaction region.

voltage of the forward wave (coupling to the right) and the distance of the interaction region is a function of the distance of the interaction region.

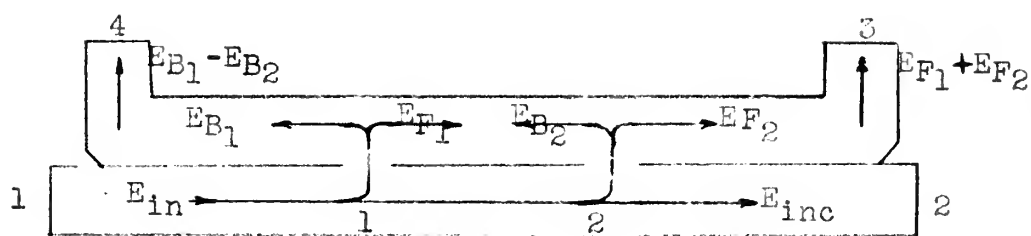
through coupling element 2. The distance of the interaction region is a function of the distance of the interaction region.

and will therefore be a function of the distance of the interaction region. The distance of the interaction region is a function of the distance of the interaction region.

By plus sign. The distance of the interaction region is a function of the distance of the interaction region.

traveled one-half guide length. The distance of the interaction region is a function of the distance of the interaction region.

the output of element 1 will be proportional to the distance of the interaction region. The distance of the interaction region is a function of the distance of the interaction region.



DIRECTIVITY OF A BIDIRECTIONAL COUPLER

FIGURE (3)

E_{B1} and E_{B2} if all terminations are perfectly matched. If the coupling elements or holes are of equal size E_{B1} equals E_{B2} . Furthermore, if they are infinitesimally small the path difference between E_{B1} and E_{B2} is exactly $\lambda_g/2$, and no backward wave exists. Therefore, two practical limitations on perfect directivity at one given frequency (corresponding to λ_g), are hole size and longitudinal hole spacing. The problem is increasingly complex with the requirement of high directivity across a 20% bandwidth.

Several means of attaining tight coupling and high directivity over a broad band by use of multipath directional couplers will now be discussed in order to determine the design criteria of not only aperture^{*} shape and size, but also aperture location.

2. Coupling

Coupling can be obtained in many ways through variously sized and shaped apertures. The apertures may be placed in either the small or the large dimension of the guide; and they may be located in various positions transversely and longitudinally along the guide and with respect to each other. Each of these dimensions mentioned are very critical and must be accurately computed and machined.

The first limitation placed on coupling elements is physical. Obviously they can be no larger than the dimensions of the guide. Also the size must be limited in order to make the small hole theory¹ valid.

*Coupling apertures are an obvious choice over probes and loops since the physical placement of the latter presents a problem.

Several means of obtaining the required information have been suggested. The first is to obtain the information from the records of the various departments of the Government. The second is to obtain the information from the records of the various departments of the Government. The third is to obtain the information from the records of the various departments of the Government.

2014-2015

1. The first thing I noticed when I stepped out of the plane was the cold, crisp air. It felt like a blanket after a long, hot journey. The ground below was a vast, flat expanse of white, stretching out to the horizon. The sun was low in the sky, casting a golden glow over the entire scene. I took a deep breath, savoring the fresh air. The silence was absolute, broken only by the distant hum of the plane's engines. I felt a sense of peace and tranquility that I had never experienced before. The world seemed so small and so quiet, as if everything was just beginning. I smiled to myself, knowing that this was the start of a new adventure. The journey ahead was long, but I was ready for it. The first step had been taken, and I was moving forward. The world was my oyster, and I was about to open it. The journey was just beginning, and I was excited to see what it had in store for me. The first step had been taken, and I was moving forward. The world was my oyster, and I was about to open it. The journey was just beginning, and I was excited to see what it had in store for me.

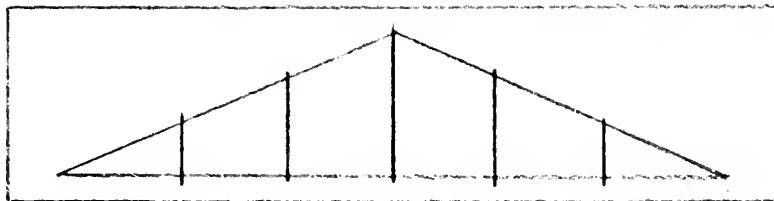
• 551 •

the physical elements of the system are not the same as the physical elements of the system.

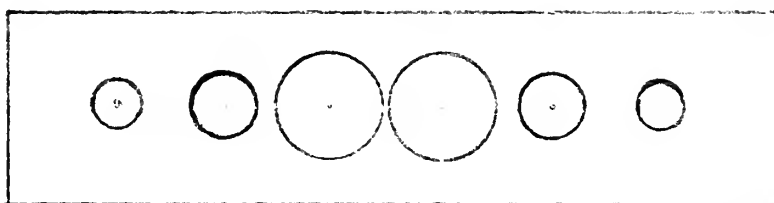
The small hole theory will be discussed extensively in Chapter III. Working with small x-band wave guide, which supports frequencies from 8.2 to 12.4 KMC/sec, it has been shown² that the small hole theory was reasonably accurate up to hole diameters of .350 inches.

Miller and Mumford³ achieved tight coupling up to complete transmission into the auxiliary guide by means of a long slot. Use was made of the 90° phase delay experienced when coupling from the main to the auxiliary guide, along with a second 90° phase delay resulting from coupling from the auxiliary to the main guide at the next aperture. The severe reflections normally encountered in slot couplers were avoided by placing wires transversely across the slot. These served to suppress the higher modes. Figure (4) illustrates this type coupling. This in effect divided the slot into several apertures. The small guide dimension was used for coupling. Both theoretical and experimental results show this type coupling to be frequency sensitive.

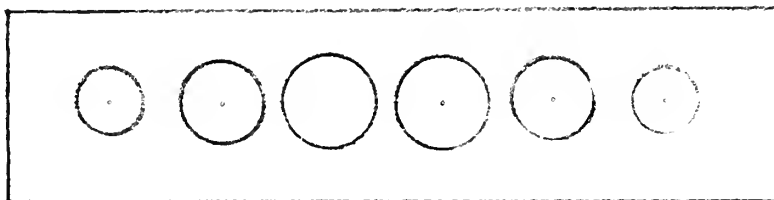
A second coupling theory using the binomial array type coupler was first introduced by Harrison⁴ and later used by Mumford.⁵ Each successive hole of a binomial coupler couples a voltage which is proportional to the coefficients of the terms of the binomial expansion to the $2N-1$ power where $2N$ is the total number of elements. This array must use holes which are small enough to make the small hole theory valid in order to predict its performance. However, either face of the guide may be used for the coupling. If the large is used, the coupling across the band will be reasonably flat since



Miller-Mumford



Binomial



Tchebyscheff

COUPLING ELEMENT TAPER

FIGURE (4)

the frequency dependent part of the coupled voltage as shown later in equation (16), Chapter III is $(\frac{\lambda_g}{2d} + \frac{2d}{\lambda_g})$. The source of this term will be shown in the next chapter.

A third approach to obtaining the tight coupling required involves the use of Dolph's⁶ antenna theory. It is similar to the binomial array coupler except that the voltage coefficients are made proportional to the normalized coefficients of the Tchebyscheff polynomial of order $(2N-1)$ where $2N$ is the total number of elements. This multi-element array may be coupled on either face of the guide. The size of the holes will be limited not only by the physical dimensions but also by the small hole theory.

It was decided that the optimum shape of the apertures of either the binomial or the Tchebyscheff type couplers was round since this could be more easily machined than other odd shapes and still maintain tolerances. A double row of small coupling holes, would double the voltage coupling capability, i.e., increase voltage coupling by 6 db. Since the holes must be small to make the small hole theory valid and since the broad dimension will be used for coupling, this does not place too stringent physical limitations on the hole diameters. For small x-band, the internal guide dimensions are 0.9×0.4 ". For a doubled row of coupling holes, therefore, the largest possible radius of a coupling hole is $.225$ ", or a diameter of $.450$ ". Since hole sizes must be limited to less than $.350$ " in order to apply the small hole theory in the small x-band region, the above mentioned physical limitation is not significant.

3. Directivity

The most obvious and universally used method of obtaining broadband directivity is that of varying the size of the coupling elements. This is known as taper. Figure (4) illustrates the methods of tapering used in the three previously discussed couplers. Also directivity increases directly with an increase in coupling elements. The limitation to this is the total practical length of a coupler.

Miller and Mumford point out that the backward wave in a coupler is related to the shape of the coupling slot by the Fourier transform.

$$I_b = F \int_{-L/2}^{+L/2} \varphi(z) e^{-j(4\pi/\lambda g)z} dz \quad (2)$$

$$\text{and } I_f = F \int_{-L/2}^{+L/2} \varphi(z) dz \quad (3)$$

L is total length of coupling slot

z is the longitudinal dimension of the guide

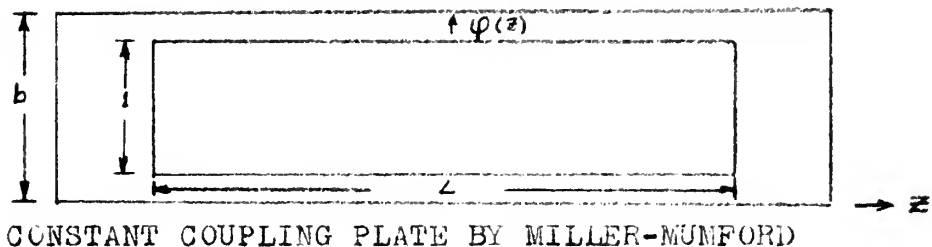
$\varphi(z)$ is the shape of the coupling function

b is the small dimension of the guide

If the coupling were uniform over the interval of coupling, L , i.e.,

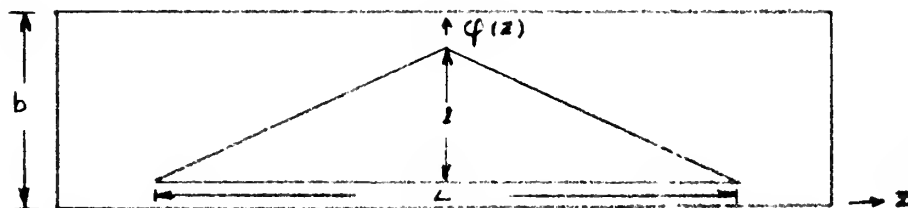
$\varphi(z)$ equals one as shown in figure (5), then the directivity is given as

$$D = \frac{I_f}{I_b} = \frac{F \int_{-L/2}^{+L/2} (1) dz}{F \int_{-L/2}^{+L/2} (1) e^{-j(4\pi/\lambda g)z} dz} \quad (4)$$



CONSTANT COUPLING PLATE BY MILLER-MUMFORD

FIGURE(5)



TAPERED COUPLING PLATE BY MILLER-MUMFORD

FIGURE(6)

Integrating and substituting the identity $\sin x = \frac{e^{jx} - e^{-jx}}{2j}$

$$D = \frac{L}{\frac{\sin(2\pi L/\lambda_g)}{2\pi/\lambda_g}} = \frac{2\pi L/\lambda_g}{\sin(2\pi L/\lambda_g)} \quad (5)$$

Plotting directivity as a function of L/λ_g , it was found that high theoretical directivities were attained after a length, L , of 2 to 3 wave-lengths.

When the coupling function (z) was tapered as shown in figure (6), higher directivities for a given length, L , were attained when compared with the above constant coupling function. Actual measurements³ of directivity made were found to be in close accord with this theory. However, this theory is presented with directivity as the primary object, and the coupling was loose and not easily determined theoretically in addition to being frequency sensitive. Coupling the large dimension with this tapered slot would eliminate the frequency sensitivity objection. However, it is felt that this interruption of the E-field would give results which could not be predicted by the small hole theory. Nevertheless, this is a practical approach and will undoubtedly be successfully applied in the future. Time did not permit a deeper investigation of its possibilities.

The binomial array is capable of giving very high directivity if enough holes are used. The theoretical directivity versus frequency plot of this type coupler will result in infinite directivity at the design frequency, f_0 . The directivity is still high very close to f_0 but becomes increasingly worse the farther it is removed.

Plotting the results as a function of ω , the results are shown in Fig. 1. The high ω or short duration limit was calculated using the asymptotic expansion of the wave function.

From the results of Fig. 1, it is seen that the coupling constant λ is of the order of 10^{-2} for the high ω limit, and the coupling constant λ is of the order of 10^{-1} for the low ω limit.

It is interesting to note that the results of this theory, however, are in good agreement with the results of the exact calculation.

The present theory, and the coupling constant λ are of the order of 10^{-2} for the high ω limit, and the coupling constant λ is of the order of 10^{-1} for the low ω limit.

The large ω limit is of the order of 10^{-2} for the high ω limit, and the coupling constant λ is of the order of 10^{-1} for the low ω limit.

Of the small ω limit, the results are in good agreement with the results of the exact calculation.

Small ω limit theory, however, is in good agreement with the results of the exact calculation.

It is interesting to note that the results of this theory, however, are in good agreement with the results of the exact calculation.

The present theory, and the coupling constant λ are of the order of 10^{-2} for the high ω limit, and the coupling constant λ is of the order of 10^{-1} for the low ω limit.

The large ω limit is of the order of 10^{-2} for the high ω limit, and the coupling constant λ is of the order of 10^{-1} for the low ω limit.

With a Tchebyscheff array⁶, the directivity is theoretically infinite at several frequencies across the suppression band. This occurs with an oscillatory action which is a function of the order of the Tchebyscheff polynomial. Possibly it is easier to explain the directivity when working with an antenna pattern as illustrated by Dolph. A zero side lobe radiation can be compared with a zero backward wave (infinite directivity). In the terminology of a directional coupler, a coupler which has $2N$ coupling elements which couple voltage in proportion to the coefficients of a Tchebyscheff polynomial of order $2N-1$, will have a computed backward wave which will oscillate about zero with a ripple of constant magnitude across the designed suppression band. Thus a Tchebyscheff array has a maximum error which is independent of frequency while the backward voltage of a binomial array is a function of frequency.

[illegible]

CHAPTER III

THEORETICAL DESIGN

After weighing the above-mentioned considerations of coupler design, it was decided to attempt to design and build a Tchebyscheff small hole type coupler with -3db coupling and 40 db directivity across the frequency band of 8 to 10 kmc/sec. The large dimension was used for coupling in order to take advantage of the 6 db gain in coupling two rows of small holes, as well as obtaining relatively frequency insensitive coupling. In addition advantage can be made of the inherent directivity which will be discussed later.

Bethe's¹ small hole theory is valid if the following limitations are imposed:

- (1) the coupling hole is much less than λ_g
- (2) the holes are in an infinitely thin wall
- (3) that the holes are far from corners, and
- (4) that measurements are made far enough from the holes that the higher order modes excited there have been damped out.

Assuming that these limitations are satisfied, we can make use of the following expressions:

$$E_z = \sum_{n=1}^{2N} A_n \quad (6)$$

$$E_y = \sum_{n=1}^{2N} B_n \cos(2n-1)\beta z \quad (7)$$

or due to symmetry

$$E_z = 2 \sum_{n=1}^N A_n \quad (8)$$

$$E_y = 2 \sum_{n=1}^N B_n \cos(2n-1)\beta z \quad (9)$$

where E_3 and E_4 are the outputs as shown in figure (2)

$2N$ is number of longitudinally distinct coupling holes

A_n is the forward coefficient of coupling for coupling hole n

B_n is the backward coefficient of coupling for coupling hole n

$n = 1, 2, 3, 4, \dots, N$

$$\beta = 2\pi/\lambda_g$$

z is the longitudinal coordinate of the guide

Equation (8) merely says that the voltage coupled in the forward direction is equal to the sum of all the voltages coupled by the individual apertures. Equation (9) states the same thing for the backward voltage but has the directional factor introduced by virtue of path difference.

Now considering the Tchebyscheff polynomials as defined by⁷

$$T_m(x) = \cos(m \cos^{-1} x) \quad -1 < x < +1 \quad (10)$$

$$T_m(x) = \cosh(m \cosh^{-1} x) \quad |x| > 1 \quad (11)$$

If x equal to $\cos \beta z$ is substituted for the argument of equation (10), it becomes

$$T_m(\cos \beta z) = \cos m \beta z \quad \text{for} \quad \pi > \beta z > 0 \quad (12)$$

with $m = (2n-1)$, equation (12) is in the form of equation (9) since the expansion of equation (12) contains only terms in $\cos(2n-1)\beta z$ and the terms end with $n=N$. Therefore, if the backward coefficients

where \mathbf{I}_0 and \mathbf{I}_1 are the identity matrices of order n and $n-1$ respectively. \mathbf{I}_0 is the identity matrix of order n and \mathbf{I}_1 is the identity matrix of order $n-1$. \mathbf{I}_0 is the identity matrix of order n and \mathbf{I}_1 is the identity matrix of order $n-1$. \mathbf{I}_0 is the identity matrix of order n and \mathbf{I}_1 is the identity matrix of order $n-1$.

$$\mathbf{I}_0 = \begin{pmatrix} 1 & 0 & \dots & 0 \\ 0 & 1 & \dots & 0 \\ \vdots & \vdots & \ddots & \vdots \\ 0 & 0 & \dots & 1 \end{pmatrix}$$

is the longitudinal component of the electric field. Equation (8) merely says that the electric field in the longitudinal direction is equal to the sum of all the voltage drops of the individual segments. Equation (9) states that the voltage drops are equal to the backward voltage but the directional derivative is taken in the direction of the electric field.

Now considering the forward and backward components of the electric field

$$\mathbf{E}_f(x) = \cos(\alpha x) \mathbf{E}_0(x) \quad (10)$$

$$\mathbf{E}_b(x) = \cos(\alpha x) \mathbf{E}_0(x) \quad (11)$$

if x equal to zero the backward component is zero and the forward component is $\mathbf{E}_0(x)$. If x becomes

$$\mathbf{E}_f(x) = \cos(\alpha x) \mathbf{E}_0(x)$$

with $\alpha = \pi/L$, equation (10) is $\mathbf{E}_f(x) = \cos(\pi x/L) \mathbf{E}_0(x)$ and the expansion of equation (11) is $\mathbf{E}_b(x) = \cos(\pi x/L) \mathbf{E}_0(x)$ and the error and the n th order term is $\mathbf{E}_0(x)$.

of coupling, B_n , can be made proportional to the corresponding coefficients of the Tchebyscheff polynomial of order $2N-1$, the theoretical directivity will have a suppression band of equal-ripple magnitude. These coefficients are developed in Appendix (B).

Now a design parameter, z_0^6 , which determines the width of the suppression band, must be established. The value of 1500:1 for a ratio of forward to backward waves was chosen. This gives a $D=63.5$ db which was considered to be sufficient overdesign. Equation (13) determines z_0 as follows:

$$z_0 = \frac{1}{2} \left[(g + \sqrt{g^2 - 1})^{1/m} + (g - \sqrt{g^2 - 1})^{1/m} \right] \quad (13)$$

In this equation, m is equal to $2N-1$; the value of $2N$ was established at 10 as a good compromise to limit hole size and still attain -3 db coupling. In addition the higher order Tchebyscheffs become difficult to manipulate mathematically. Thus for $g=1500$ and $m=9$, equation (13) was solved and z_0 was found to be 1.42.

With this value of z_0 , the coefficients of a Tchebyscheff polynomial of order 9 were solved for. See Appendix (B). Making the coefficients of coupling proportional to the Tchebyscheff coefficients, and solving for hole size (this method to be shown later) resulted in the fact that for -3db coupling the holes would overlap. However, this overlap result produced the idea of superimposition^{2,4} of coupling coefficients to attain a reasonable size hole with the degree of coupling required. The result was the superimposition of four ten element arrays which resulted in a 22 element superimposed

Tehebyscheff type array. See Appendix (B) and figure (7).

From Appendix (B), the total of all the Tehebyscheff coefficients, T_t , for the 44 coupling holes (two rows of 22) is 476.16. The total coupling ratio, A_t , for -3 db coupling is

$$Cdb = 20 \log A_t \quad A_t = .708 \quad (14)$$

The Tehebyscheff coefficients for the individual holes, T_n , are tabulated in Appendix (B). Therefore, the forward coefficient of coupling for each individual hole, A_n , can be determined by solving the following simple ratio:

$$2x \frac{A_n}{A_t} = \frac{T_n}{T_t} \quad (15)$$

It may be noted that n needs to run only from 1 to 11 since the array is longitudinally symmetrical, and the pairs of holes located in the same transverse position are of the same size, as shown in figure (8).

From the small hole theory¹, the following expressions are for the forward voltage coefficient and the backward voltage coefficient, respectively, of one individual hole; n .

$$A_n^* = j \frac{2\pi r_n^3}{3a^2b} \left\{ \alpha_E \left(\frac{a}{\lambda_g} + \frac{\lambda_g}{2a} \right) \sin^2 \frac{\pi x_n}{a} - 2\alpha_H \left(\frac{a}{\lambda_g} \right) \sin^2 \frac{\pi x_n}{a} - 2\alpha_H \left(\frac{\lambda_g}{2a} \right) \cos^2 \frac{\pi x_n}{a} \right\} \quad (16)$$

$$B_n^* = j \frac{2\pi r_n^3}{3a^2b} \left\{ \alpha_E \left(\frac{a}{\lambda_g} + \frac{\lambda_g}{2a} \right) \sin^2 \frac{\pi x_n}{a} + 2\alpha_H \left(\frac{a}{\lambda_g} \right) \sin^2 \frac{\pi x_n}{a} - 2\alpha_H \left(\frac{\lambda_g}{2a} \right) \cos^2 \frac{\pi x_n}{a} \right\} \quad (17)$$

*These are developed in Appendix A.

... of the ...
 ... (2) ...
 ...
 The ...

...
 ...
 ...
 ...
 the ...



(1)
$$\frac{dx}{dt} = \frac{dx}{dt} \cdot \frac{dt}{dx}$$

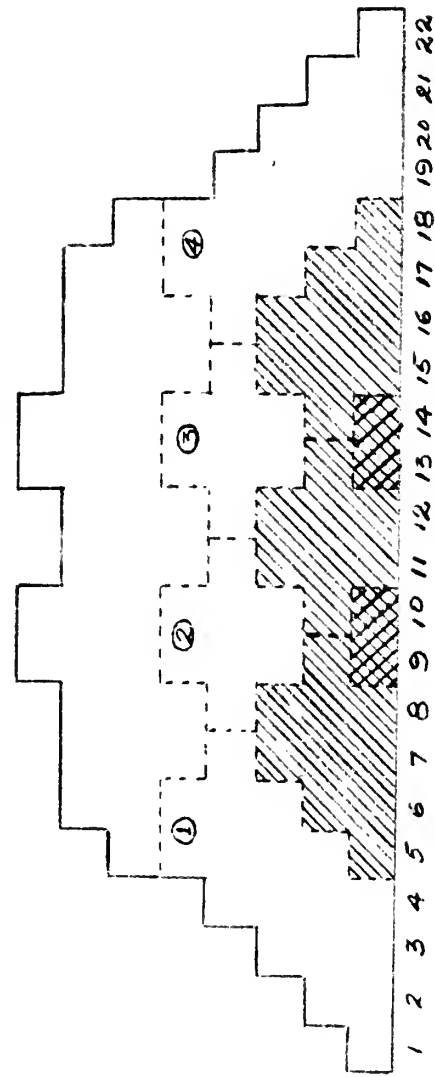
It may be ...
 ...
 ...
 ...
 the ...
 ...

(2)
$$\frac{dy}{dx} = \frac{dy}{dx}$$

... (3) ...

Superimposed Tchebyscheff
Coefficient, T_3
29.77
29.75
28.77
25.35
18.82
10.93
4.42
1.00

-  TWO "10 ELEMENT ARRAYS" SUPERIMPOSED
-  THREE "10 ELEMENT ARRAYS" SUPERIMPOSED
- OUTLINE OF 4 ARRAYS SUPERIMPOSED
- OUTLINE OF A SINGLE 10 ELEMENT ARRAYS
- ① A SINGLE 10 ELEMENT ARRAY



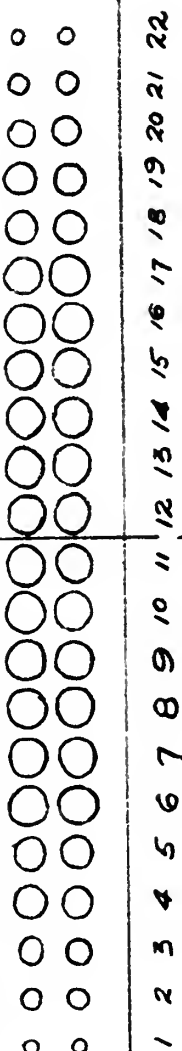
SUPERIMPOSED TCHEBYSCHIEFF COEFFICIENTS IN PARNETT

FIGURE (7)

COUPLING PLATE, FINAL DESIGN FOR 3 DB COUPLING
40 DB DIRECTIVITY

LINE
OF
SYMMETRY

1/2 IN



$$\chi_1 = .225''$$

THEORETICAL	MEASURED
diameter 1 = .121	.121
" 2 = .184	.184
" 3 = .240	.238(1)
" 4 = .282	.281(1)
" 5 = .308	.3045(2)
" 6 = .320	.321(1)
" 7-11 = .324	.323(20)

FIGURE (8)

where a large inner dimension of the guide
 b small inner dimension of the guide
 r radius of the coupling hole
 λ_g guide wave-length
 x_1 distance from side of guide to the center of the coupling hole
 z_1 spacing center to center between holes
 α_g electric field attenuation factor due to guide thickness

See figure (9)

The three terms in the brackets arise from the electric field, the transverse component of the magnetic field, and the longitudinal component of the magnetic field, respectively. These are complex relations which are very unwieldy unless some simplifying assumptions are made. If the variables of equation (16) can be separated by legitimate approximations a coupling design may be established.

The variables α_e and α_h are attenuation factors due to the finite wall thickness in which the holes are drilled. By use of these factors, limitation (2) on page 16 is no longer a restriction. These holes are considered as circular wave guides below cutoff. The electric field term from equation (16) sets up a TM_{01} mode, while the magnetic field corresponds to the TE_{11} mode. Since the TM_{01} mode is farther below cutoff, it is attenuated more than the TE_{11} mode. Therefore, the coefficient of attenuation for the

AD-68-907

1. The first of these is the fact that the

and 3. However, it is arbitrary to

2000-2001

... to this work ...
... and ...

1. The first step is to identify the problem or question that needs to be answered.

THE NATIONAL ARCHIVES COLLEGE PARK, MARYLAND

1957

The three centers in the Southwest are the Southwest Center for the Study of the American Indian, the Southwest Center for the Study of the American Indian, and the Southwest Center for the Study of the American Indian. The Southwest Center for the Study of the American Indian is the largest of the three centers and is located in the Southwest Center for the Study of the American Indian. The Southwest Center for the Study of the American Indian is the largest of the three centers and is located in the Southwest Center for the Study of the American Indian. The Southwest Center for the Study of the American Indian is the largest of the three centers and is located in the Southwest Center for the Study of the American Indian.

The variation of the magnetic field with distance from the surface of the earth is shown in Figure 1. The magnetic field is a vector quantity and its direction is indicated by the arrow. The magnitude of the field is indicated by the length of the arrow. The field is a function of distance from the surface of the earth and is a function of the latitude of the observation point. The field is a function of the time of day and is a function of the season of the year. The field is a function of the magnetic activity of the sun and is a function of the magnetic activity of the earth. The field is a function of the magnetic activity of the moon and is a function of the magnetic activity of the planets. The field is a function of the magnetic activity of the stars and is a function of the magnetic activity of the galaxies. The field is a function of the magnetic activity of the universe and is a function of the magnetic activity of the multiverse.

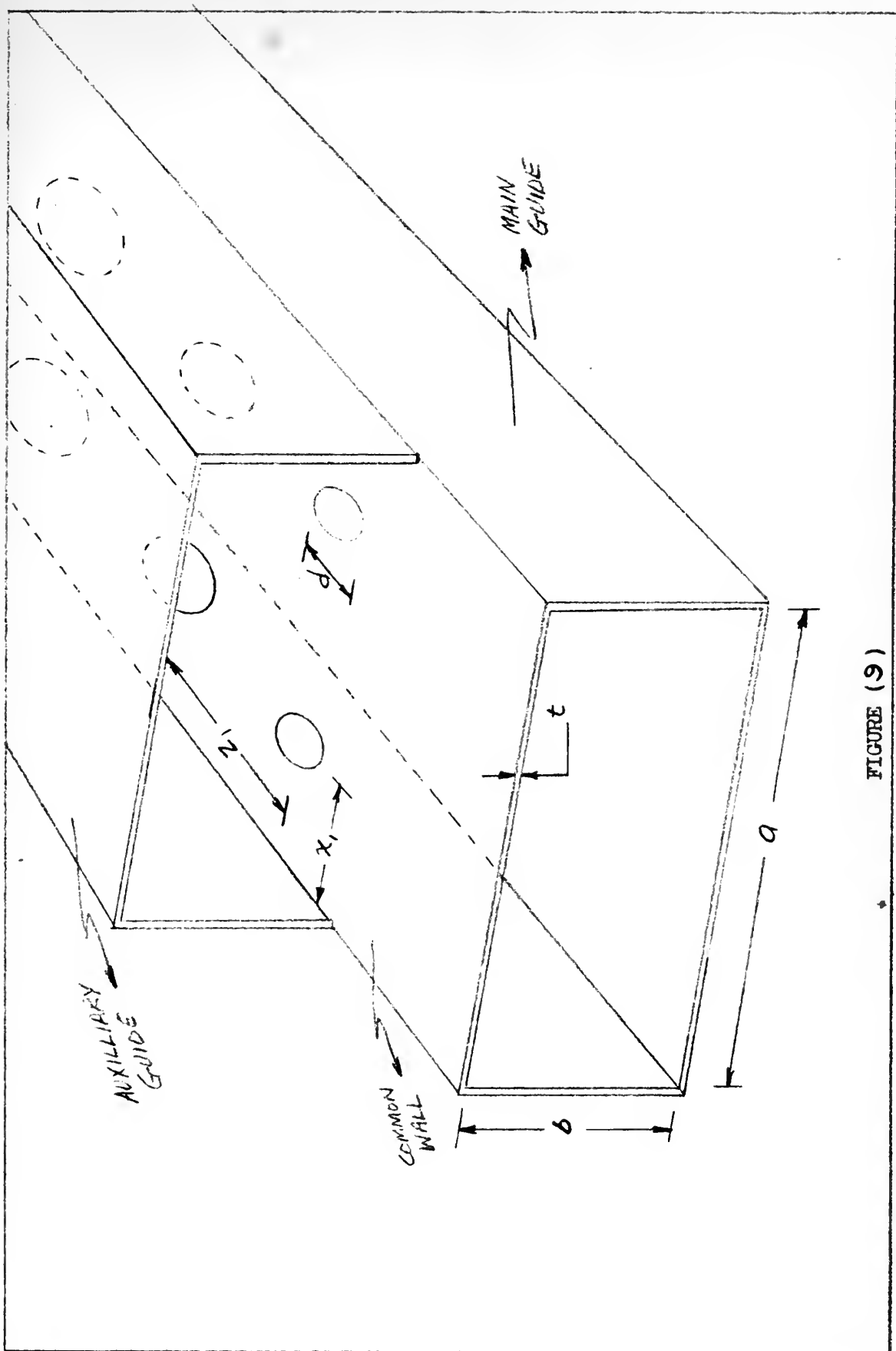


FIGURE (9)

magnetic field α_H is larger than the coefficient α_E .

$$\alpha_E(\rho, \lambda) = e^{-2.405 t/r [1 - (2.613 \rho)^2]^{1/2}} \quad (18)$$

$$\alpha_H(\rho, \lambda) = e^{-1.841 t/r [1 - (2.412 \rho)^2]^{1/2}} \quad (19)$$

where ρ is a geometry factor which varies with the thickness, t , of the common wall and the radius, r , of the hole. λ is free space wavelength. (See figure (9)).

The first approximation made in the small hole theory, equations (16) and (17) follows. Expanding the radical in the exponent of α_E by the binomial theorem expansion, the second order and higher terms may be thrown out. Therefore equations (18) and (19) become functions of ρ alone; and further, upon fixing a value for the common wall thickness, α_E and α_H become functions of the radius alone. Then equations (18) and (19) become

$$\alpha_E(\rho) = e^{-2.405 t/r} \quad (20)$$

$$\alpha_H(\rho) = e^{-1.841 t/r} \quad (21)$$

This first order approximation is a help in simplification; however, the variables r and λ are still not separable in equation (16). Thus a second approximation is introduced. Since the α_H term appears in two terms and α_E appears in one term of equation (16) a weighted attenuation factor will give a closer approximation than the use of the predominant α_H .

(1)

1.

whereas the above mentioned conditions are not satisfied,

of the system will be the same as that of the system

space within the system.

The first condition is that the system is not

tion (16) and (17) which are the conditions of the system

of the system is the same as that of the system

terms may be shown to be the same as that of the system

found in the system, and the system is the same as that of the system

common well known, and the system is the same as that of the system

then the system (17) is the same as that of the system

(1)

(1)

the system is the same as that of the system

however, the system is the same as that of the system

(16). The second condition is that the system is the same as that of the system

form appears in the system, and the system is the same as that of the system

a system is the same as that of the system

the case of the system.

Therefore, let equations (20) and (21) become

$$\alpha_E(\rho) = \alpha_H(\rho) = \alpha_{EH}(\rho) = e^{-2.029t/r} \quad (22)$$

Now the λ_g terms and the r terms of equation (16) may be separated. The forward coupling coefficient can now be written in the following forms:

$$A(\rho, \lambda_g) = \frac{2\pi r^3}{3a^2b} \alpha_{EH} \left\{ \left(\frac{2a}{\lambda_g} + \frac{\lambda_g}{2a} \right) \sin^2 \frac{\pi x_1}{a} - \left(\frac{2a}{\lambda_g} \right) 2 \sin^2 \frac{\pi x_1}{a} - \left(\frac{\lambda_g}{2a} \right) 2 \cos^2 \frac{\pi x_1}{a} \right\} \quad (23)$$

$$|A(\rho, \lambda_g)| = |K(\rho)| \cdot |F_A(\lambda_g)| \quad (24)$$

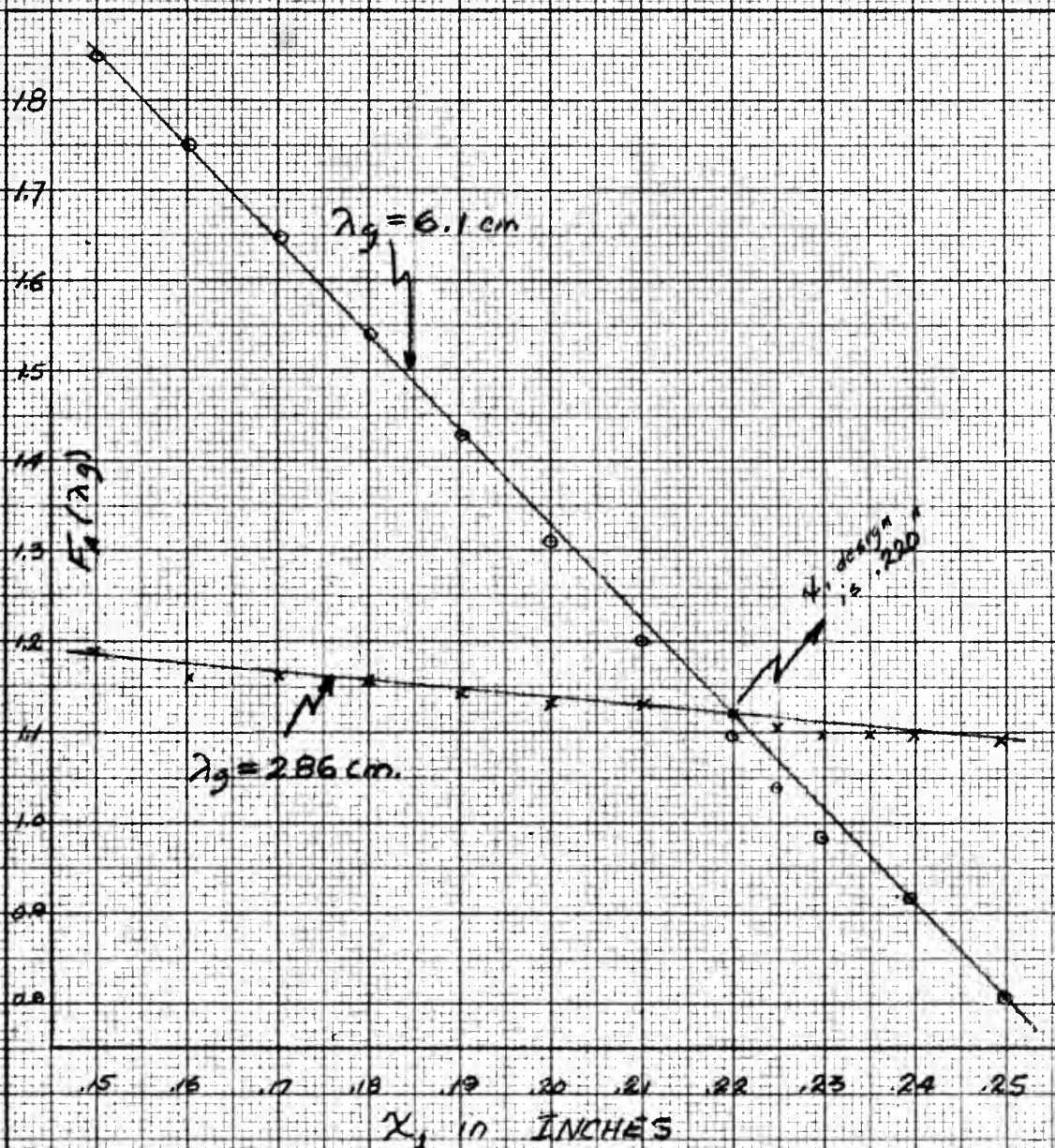
where

$$|F_A(\lambda_g)| = \left\{ \left(\frac{2a}{\lambda_g} + \frac{\lambda_g}{2a} \right) \sin^2 \frac{\pi x_1}{a} - 2 \left(\frac{2a}{\lambda_g} \right) \sin^2 \frac{\pi x_1}{a} - 2 \left(\frac{\lambda_g}{2a} \right) \cos^2 \frac{\pi x_1}{a} \right\} \quad (25)$$

$$|K(\rho)| = \frac{2\pi r^3}{3a^2b} \alpha_{EH}(\rho) = \frac{2\pi r^3}{3a^2b} e^{-2.029t/r} \quad (26)$$

The value of x_1 was established by plotting $|F_A(\lambda_g)|$ vs. x_1 at the two extremities of λ_g for small x-band guide. (Figure (10)) This will give the least deviation of coupling across the band. The intersection of these two curves established x_1 at 0.22 inches.

The design value of λ_g was established from a plot of $|F_A(\lambda_g)|$ vs. λ_g . A horizontal line was drawn at the mean value of $|F_A(\lambda_g)|$. In the final plot of coupling this will coincide with -3 db. This mean existed for two separate values of λ_g . The smaller λ_g was chosen in order to make the overall length of the coupler less. $\lambda_{g \text{ design}}$ was



$F_A(\lambda_g)$ vs. X_1

FIGURE (10)

established in this manner at 3.24 cm ($z_1 = .319''$). See design figure (11). It will be shown later that z_1 had to be increased. It was finally established at .350".

The value of equation (25) at the design frequency ($\lambda_g/4 = .350$) is a constant, i.e.,

$$|F_A(\lambda_g)|_{1.40''} = 1.05 \quad (27)$$

From equation (24)

$$|A(\rho)|_{\lambda_g=1.40''} = 1.05 K(\rho) = 1.05 \times \frac{2\pi r^3}{3a^2 b} e^{-2.029 t/r} \quad (28)$$

For $t = .025''$, $a = .9''$, and $b = .4''$, equation (28) becomes

$$|A(r)_n| = 6.79 r_n^3 e^{-.046/r_n} \quad (29)$$

By inspection of equation (17), it is seen that

$$|B(\rho, \lambda_g)| = |K(\rho)| \cdot |F_B(\lambda_g)| \quad (30)$$

where

$$|F_B(\lambda_g)| = \left\{ \left(\frac{za}{\lambda_g} + \frac{\lambda_g}{2a} \right) \sin^2 \frac{\pi z}{a} + 2 \left(\frac{za}{\lambda_g} \right) \sin^2 \frac{\pi z}{a} - 2 \left(\frac{za}{2a} \right) \cos^2 \frac{\pi z}{a} \right\} \quad (31)$$

$$|F_B(1.40'')| = 1.44 \quad (32)$$

$$|B(r)_n| = 9.30 r_n^3 e^{-.046/r_n} \quad (33)$$

Equations (29) and (33) are identical except for a constant coefficient. In order to get the correct coupling, the $A(r)_n$'s

established in this manner at 3.33 or at 3.34.

Figure (11) is a plot of $\log \frac{1}{1 - \alpha}$ versus $\log \frac{1}{1 - \alpha}$.

It was similarly established at 3.34.

The value of $\log \frac{1}{1 - \alpha}$ at the origin is 0.

in a logarithmic scale.

From equation (34)

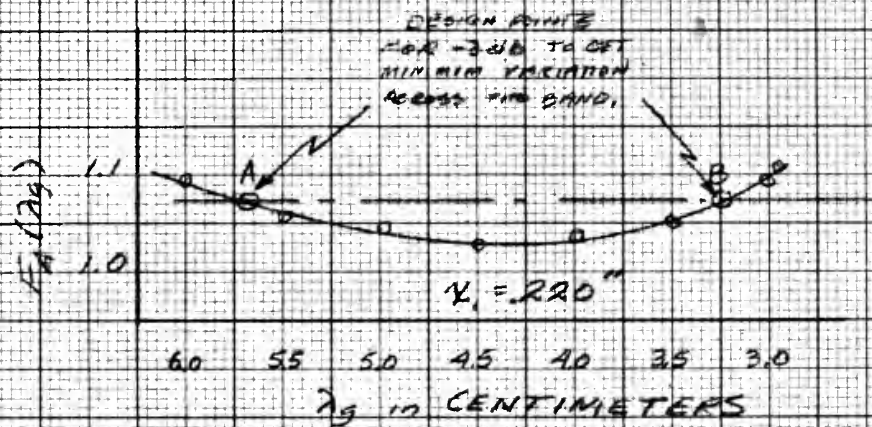
For $\alpha = 0.01$, $\log \frac{1}{1 - \alpha} = 0.01005$, and for $\alpha = 0.02$, $\log \frac{1}{1 - \alpha} = 0.02020$.

By inspection of curve (IV), it is seen that

where

Equation (35) is a plot of $\log \frac{1}{1 - \alpha}$ versus $\log \frac{1}{1 - \alpha}$.

It was similarly established at 3.34.



$F_A(\lambda_g)$ vs. λ_g

FIGURE (11)

should be proportional to the Tchebyscheff coefficients. On the other hand if the directivity is to be of equal ripple magnitude, the $B(r)_n$'s should be set proportional to the Tchebyscheff coefficients. The coupling should be within less than 1 db of -3 db, whereas the directivity can be anything as long as it is greater than 40 db. Therefore, the $A(r)_n$'s were used as the design coefficients.

The transcendental equation (29) was solved by assuming values of r and plotting $A(r)_n$ vs. r_n where $n = 1, 2, 3, \dots, 11$, which is the number of the particular hole considered. Taking the values of A_n solved for previously by equation (15), the diameter of a particular hole may be found, by entering the plot of equation (29). This is only approximate since it is only as good as the curve can be read. This must be checked by solving equation (29) with the approximate radius to find its agreement with the true A_n . This is repeated until the required accuracy of $\pm .001''$ is obtained for the radii. The final radii values of the 44 coupling holes are shown in figure (5). Note the largest hole size is $d = .324''$. $\lambda_{g/4_{des}}$ must be greater than this to avoid overlap. Mechanical limitations require at least $.010''$ between the circumferences of the holes. This z_1 was established previously at $.319''$ to give a minimum deviation of coupling. However, since it must be increased, it was arbitrarily set at $.350''$.

Thus having established the following design parameters, the coupler is complete:

should be...
 other part of the...
 the...
 elements. The...
 where the...
 than 40...
 effect...

The...
 of...
 number of...
 solved for...
 other...
 This...
 can be...
 the...
 This is...
 for...
 are...
 the...
 before...
 holes...
 minimum...
 it was...
 that...
 computer...

- (1) small x-band guide
- (2) hole sizes, r_n , $n = 1, 2, 3, 4, \dots, 11$.
- (3) x_1 , the transverse hole position
- (4) z_1 , the longitudinal hole position, which also establishes the design frequency.

See figure (5) for the final design.

1. $\text{H}_2\text{O} \rightarrow \text{H}^+ + \text{OH}^-$ (1)

..... (1)

[illegible]

10/10/1944

• April 1977 and '69 (8) empty lot

CHAPTER IV

EXPERIMENTAL RESULTS

The above coupler was manufactured as shown in the photograph, figure (12). The specified tolerance for the diameters of holes was $\pm .001"$. Some of the holes were measured and found to be outside of this tolerance. The actual sizes are indicated in figure (8).

The experimental laboratory setup for testing this coupler is shown in the block diagram of figure (13). The measurement of coupling is straight forward. Coupling as defined in equation (8) was measured by the Hewlett-Packard 415A amplifier. A plot of coupling vs. frequency is shown in figure (14).

The directivity measurements require very exacting laboratory techniques due to the high voltage differentials measured. Referring to figure (15), note that the output mitre joint of terminal 3 has been left off. Terminal 2 and 3 are then terminated with sliding loads which are 1.05 or better across the band. By the following technique the effect of the load reflections can be eliminated. Let \vec{E}_2' and \vec{E}_3' be the reflected voltage vectors of their respective terminals.

$$\vec{E}_2' = E_2' e^{j\theta_2'} \quad (34)$$

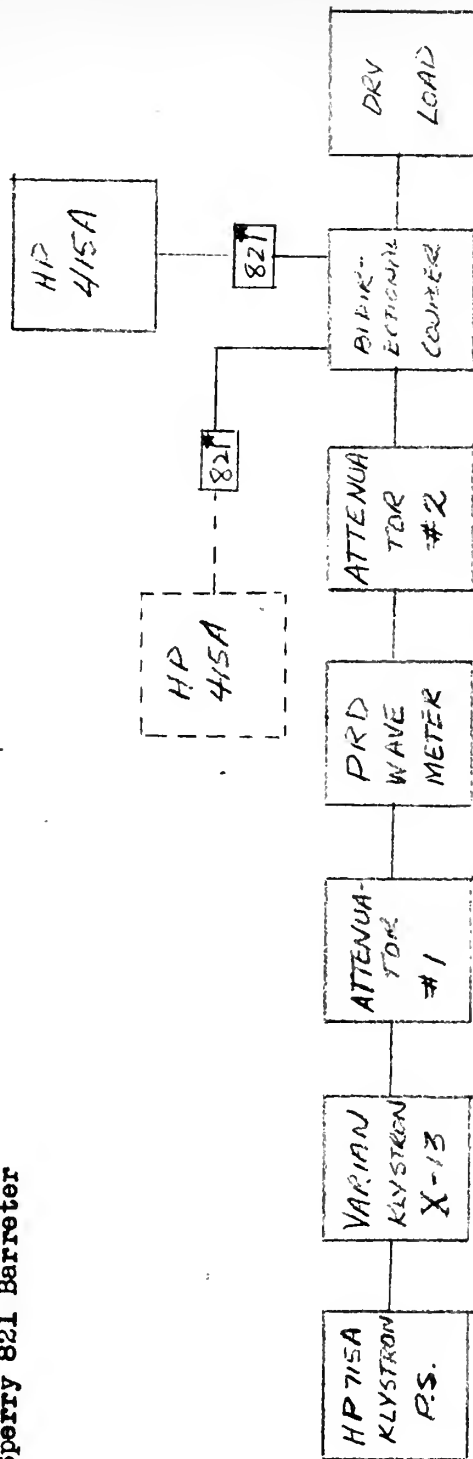
$$\vec{E}_3' = E_3' e^{j\theta_3'} \quad (35)$$

Let \vec{E}_4 be the output voltage of terminal 4 and \vec{E}_m be the portion

--- for measuring E_4 (fig 2)

— for measuring E_3 (fig 2)

* Sperry 821 Barreter



Laboratory Bench Setup for Measuring
Coupling and Directivity
of a Bi-directional Coupler

FIGURE (13)

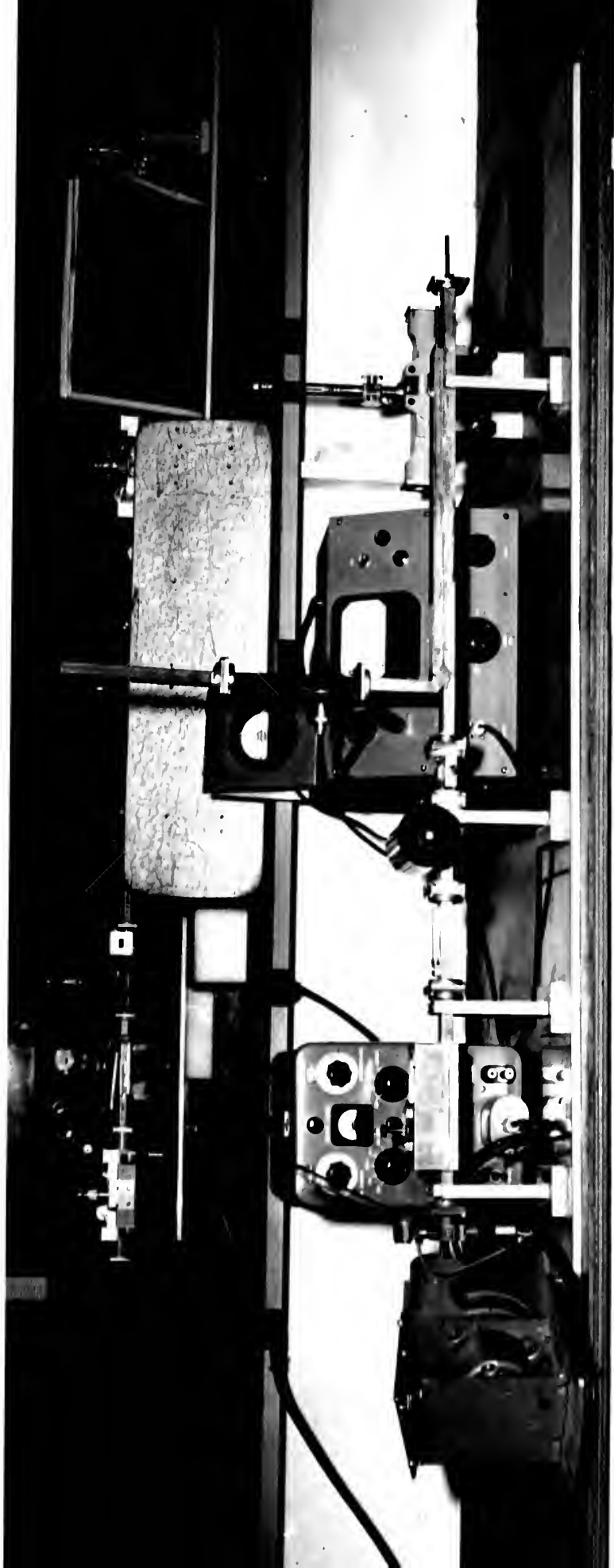
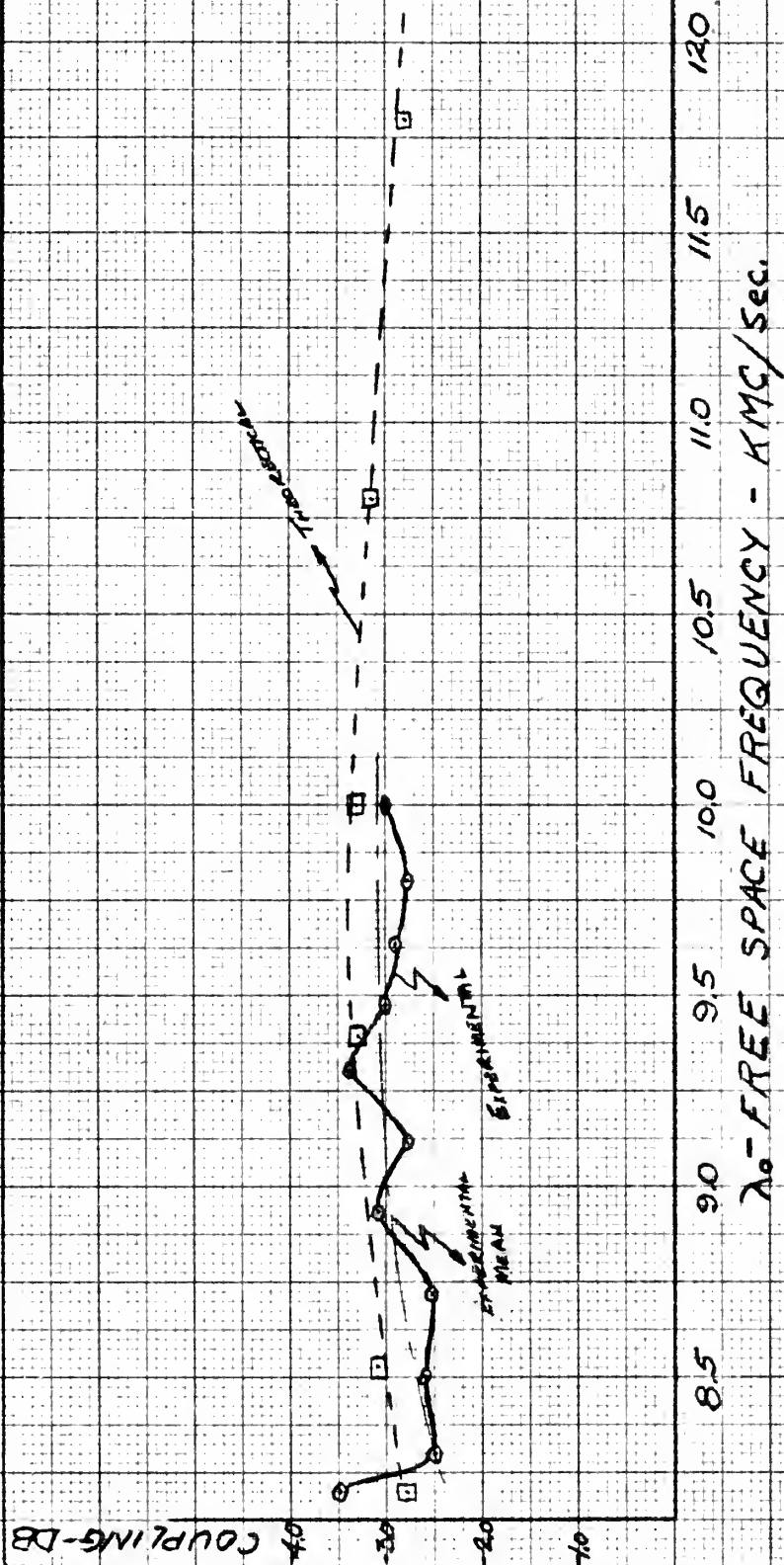
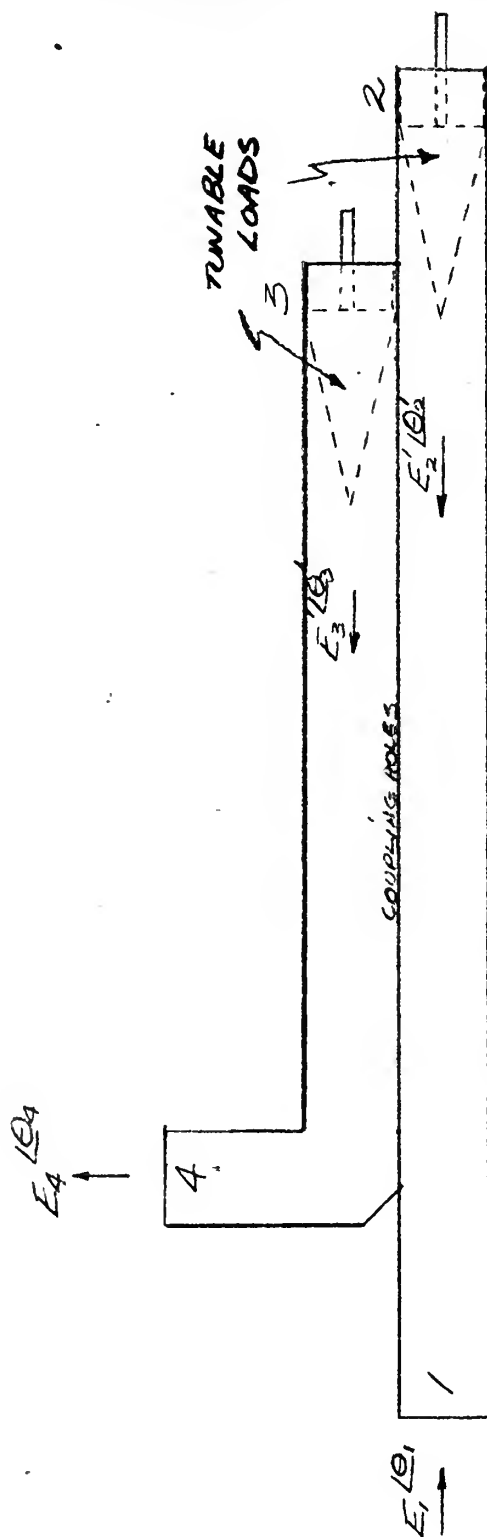


FIGURE (12)



THEORETICAL AND ACTUAL COUPLING CURVES

FIGURE (11)



An Illustration of the Technique
Involved in Measuring High
Directivities

FIGURE (15)

of \vec{E}_4 which is due to imperfect directivity. \vec{E}_m is the voltage for which we must solve.

$$\vec{E}_4 = E_4 e^{j\theta_4} \quad (36)$$

$$\vec{E}_m = E_m e^{j\theta_m} \quad (37)$$

then

$$\vec{E}_{4max} = \vec{E}_m + \vec{E}_3' + k_c^* \vec{E}_2' \quad (38)$$

If the sliding loads are carefully tuned for a maximum output signal at terminal 4, then all of the phase angles are equal and the vector magnitudes may be added directly.

$$E_{4max} = E_m + E_3' + k_c E_2' \quad (39)$$

Now tuning the two sliding loads for a minimum output reading at terminal 4, means that the phase of E_m is 180° out with the phase of E_3 and E_2 . Thus

$$E_{4min} = E_m - (E_3' + k_c E_2') \quad (40)$$

Solving these equations gives

$$E_m = \frac{E_{4max} + E_{4min}}{2} \quad (41)$$

The coupler is then reversed and the voltage output of terminal three, E_3 is measured.

*A constant less than one due to coupling

of E_4 which is the so-called "horizontal" direction. It is not possible
for which we must solve.

(10)

(11)

then

(12)

It is the sliding in the direction of the maximum stress
but signal at terminal 4, that all of the stress applied to the
and the vector magnitude of the stress is zero.

(13)

Now taking the two sliding in the direction of the maximum stress
terminal 4, means that the stress is in the direction of the
of E_3 and E_4 . Thus

(14)

Solving these equations gives

(15)

The coupled in the direction of the maximum stress and the
three, E_3 is measured.

"A constant load that is applied to the

The db difference between E_3 and E_m is the directivity, i.e.,

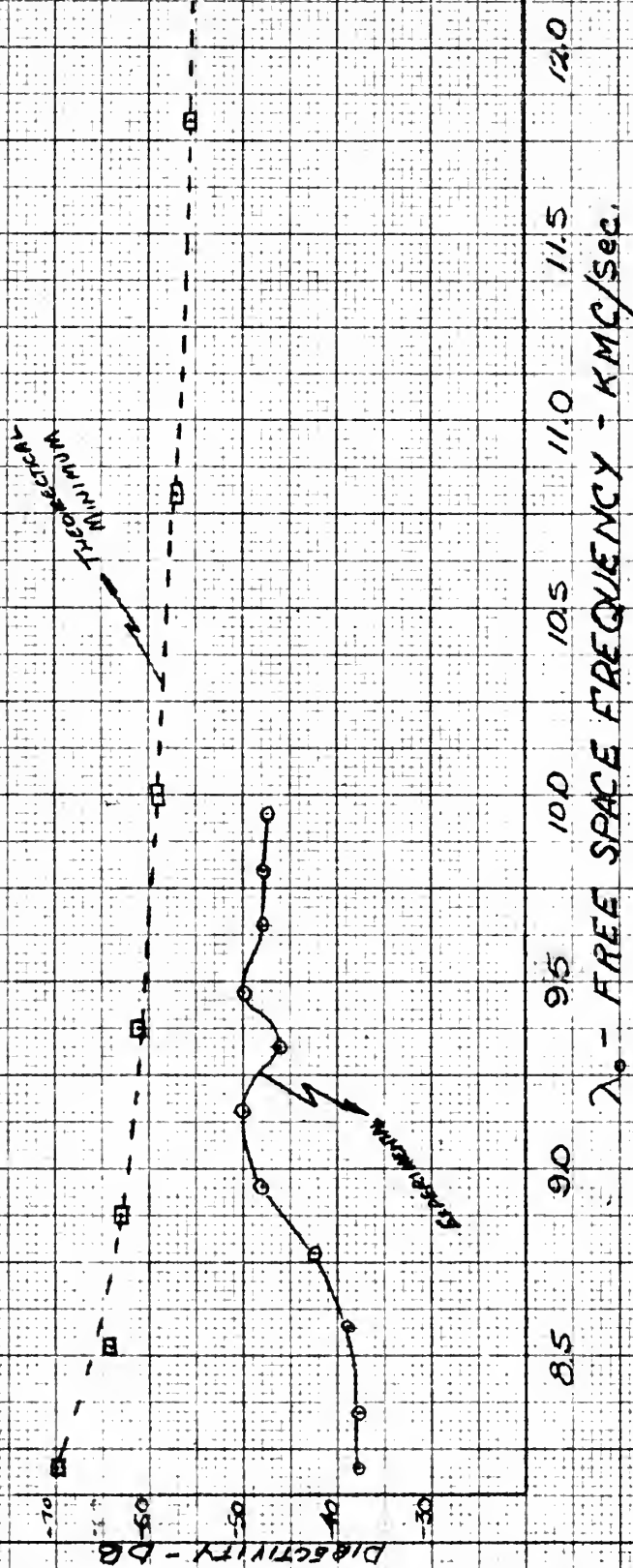
$$D = E_{3db} - E_{mdb} \quad (42)$$

A plot of this directivity vs. frequency is shown in figure (16).

The distance between the two points is 100 miles.

(1)

A plot of the data shows a linear relationship.



THEORETICAL AND ACTUAL DIRECTIVITY CURVES

FIGURE (16)

CHAPTER V

CONCLUSION

1. General

The experimental design of the bi-directional coupler has been compared with the theoretical curves, in figures (14) and (16). In general it is felt that the results have been very close to the theory. The experimental results show that the coupler has fallen slightly outside of specifications. However, it must be stated that this coupler was designed entirely theoretically. No benefit from laboratory experience was available prior to the ultimate design. It is felt that the deviations from the specifications can be justified and corrected in future models. An attempt will be made to evaluate these justifications.

2. Coupling

The theory predicted a range in coupling, as shown in figure (14) from -2.66 db at 8.2 kmc to a minimum of -3.31 db at 9.4 kmc. This gives a db difference of $.65$. The actual measured coupling ranged from -2.5 db at 8.3 kmc to -3.4 db at 9.25 kmc, or a db difference of 0.9 . The actual coupling of -3.5 db at 8.26 kmc seems to be in error, so it will not be considered. The solid red line appears to be a realistic mean for the experimental coupling. This is an average error of about -0.4 db.

The following are possible contributions to this error:

(1) Mechanical tolerances of $\pm .001''$ were requested but not obtained for the critical coupling dimensions. Such tolerances can be held. Since the radii were under size in all cases out of tolerance, this would indicate that the experimental result would show less coupling than the theoretical. This is not the overall case.

(2) The first approximation introduced a first order error as can be seen by comparison of equations (19) and (21). If second order accuracy is used, the term $\left(1 - \frac{(3.412r)^2}{(\lambda)^2}\right)^{1/2}$ becomes $\left(1 - \frac{1}{2} \left(\frac{3.412r}{\lambda}\right)^2\right)$ instead of "1", by the first order theory. The greatest error this approximation can introduce occurs when r is maximum or .411 cm and λ is minimum or 2.42 cm. The coupling using the first order theory gave -2.38 db. Thus the first order approximation has the affect of encreasing coupling, which is the overall case.

(3) The second approximation indicated in (22) is a very good one. However, it introduces a small error which makes the actual coupling tighter than the theoretical.

(4) Laboratory technique can be a random contribution to coupling measurement errors. It is estimated that the laboratory measurements are accurate to ± 0.2 db.

(5) The larger the radius of the coupling holes with respect to a wave length, the less valid is the first order theory. The largest hole diameter of this coupler is .324". This is becoming an appreciable part of a free space wave length which for 9 kmc is

1.31^m. This is an error which aggravates the second error listed above.

In consideration of these error possibilities, it is possible to reconcile partially at least, the theoretical with the experimental.

3. Directivity

As shown in figure (16), the experimental directivity has a minimum of 37.8 db at 8.26 kmc. It is below specifications from 8.26 to 8.5 kmc. There are several contributing factors.

First the theoretical directivity will be inspected. From figure (2), it is seen that

$$D = 20 \log \left| \frac{E_2}{E_1} \right| \quad (43)$$

Substituting (6) and (7) in (43)

$$D = 20 \log \frac{\sum_{n=1}^N A_n}{\sum_{n=1}^N B_n \cos(2n-1)\beta z} \quad (44)$$

Now substituting (24) and (30) into (44)

$$D = 20 \log \frac{F_A(\gamma_g)}{F_B(\gamma_g)} + 20 \log \frac{\sum_{n=1}^N K(\rho)}{\sum_{n=1}^N K(\rho) \cos(2n-1)\beta z} \quad (45)$$

The first term of (45) is a type of directivity which is inherent with any single hole. It can be either positive or negative. It gives positive directivity at the low frequencies and negative directivity at the higher frequencies. This is opposite to the error existing in this coupler.

The second term is the source of equal-ripple magnitude of reverse wave radiation. However, this optimum directivity is affected by the wide variation of the inherent directivity. But this is not the only source causing directivity to fall off.

The interactions between the holes of this multi-hole coupler in the fundamental as well as higher modes is undoubtedly a source of error. The hole sizes as stated under "coupling" above are another serious limitation, as well as the mechanical tolerances attainable.

Probably, the largest contribution to this error was made by a design error. The λ_g design used was 3.56 cm which corresponds to a frequency of 10.7 kmc. This is obviously a very poor design frequency for obtaining directivity from 8 to 10 kmc. This accounts for the drop-off in directivity at the lower frequencies, which are getting near the limit of the suppression band as determined by z_0 . A design of 4.25 would center this optimum directivity at about 9.0 kmc. This of course would lengthen the coupler considerably, but this should easily give 40 db directivity from 8 to 10 kmc.

This coupler is also a compromise in length. Greater coupling length will allow the use of more holes with a decrease in the size of the holes. This will increase both directivity and coupling accuracy.

Thus although it is very difficult to account for the results quantitatively, this qualitative discussion does give some justification to the resultant errors.

The second term is the same as the first, but the
 reverse wave reflection, however, is not
 affected by the wave variation of the
 this is not the only one causing the
 The first term is the same as the second, but
 in the fundamental as well as higher modes is
 of error. The hole sizes are small, but
 another serious limitation, as well as the
 obtainable.

Probably, the largest contribution to this error is
 a design error. The design used was 3.5t on which
 to a frequency of 10.7 Kcs. This is obviously a
 frequency for obtaining directly from 5 to 10 Kcs. This
 for the through in directivity of the lower frequencies, but
 getting near the limit of the suppression band as determined by
 a design of 4.35 would obtain this optimum directly as shown in
 time. This of course would lengthen the coupling coefficient
 this should easily give 40 or 50 dB of directivity.
 This coupler is also a good design for length, but
 length will allow the use of more holes with a 3.5t hole
 of the holes. This will increase both directivity and
 accuracy.

Thus although it is very difficult to obtain the
 quantitatively, this qualitative observation is
 location to the resultant error.

BIBLIOGRAPHY

1. Bethe, H. A. Lumped Constants for Small Irises Radiation Laboratory Report # 194, MIT, 24 March 1943.

Theory of Side Windows. Radiation Laboratory Report # 199, MIT, 4 April 1943.

Excitation of Cavities through Windows Radiation Laboratory Report # 202, 9 April 1943.

Theory of Diffraction by Small Holes, Physical Review, second series, Vol 66, Nos 7 and 8, Oct 1 and 15, pp 163-182.

Also pp 858-866 on Bethe Hole Theory of C.G. Montgomery's Techniques of Microwave Measurements, McGraw-Hill 1947, Radiation Laboratory Series # 11.
2. Barnett, E. F. of Hewlett-Packard Company, Palo Alto, California in unpublished paper.
3. Miller, S. E. and Mumford, W. W. Multi-Element Directional Couplers. Proc. of IRE Vol 40 No 9, September 1952.
4. Harrison, R. J. Design Considerations for Directional Couplers, Radiation Laboratory Report # 724, MIT 31 December 1945.
5. Mumford, W. W. Directional Couplers. Proc. of IRE, Vol 35, No 2, February 1947.
6. Dolph, C. L. A Current Distribution for Broadside Arrays which Optimize the Relationship between Beam Width and Side Lobe Level. Proc. of IRE, Vol 34, No 6, June 1946.
7. Jordan, E. C. Electromagnetic Waves and Radiating Systems. Prentice-Hall 1950, pp 440-445.

1954

... ..

... ..

1. 1941-1942 1943-1944 1945-1946 1947-1948 1949-1950 1951-1952 1953-1954 1955-1956 1957-1958 1959-1960 1961-1962 1963-1964 1965-1966 1967-1968 1969-1970 1971-1972 1973-1974 1975-1976 1977-1978 1979-1980 1981-1982 1983-1984 1985-1986 1987-1988 1989-1990 1991-1992 1993-1994 1995-1996 1997-1998 1999-2000 2001-2002 2003-2004 2005-2006 2007-2008 2009-2010 2011-2012 2013-2014 2015-2016 2017-2018 2019-2020 2021-2022 2023-2024 2025-2026 2027-2028 2029-2030 2031-2032 2033-2034 2035-2036 2037-2038 2039-2040 2041-2042 2043-2044 2045-2046 2047-2048 2049-2050 2051-2052 2053-2054 2055-2056 2057-2058 2059-2060 2061-2062 2063-2064 2065-2066 2067-2068 2069-2070 2071-2072 2073-2074 2075-2076 2077-2078 2079-2080 2081-2082 2083-2084 2085-2086 2087-2088 2089-2090 2091-2092 2093-2094 2095-2096 2097-2098 2099-2100 2101-2102 2103-2104 2105-2106 2107-2108 2109-2110 2111-2112 2113-2114 2115-2116 2117-2118 2119-2120 2121-2122 2123-2124 2125-2126 2127-2128 2129-2130 2131-2132 2133-2134 2135-2136 2137-2138 2139-2140 2141-2142 2143-2144 2145-2146 2147-2148 2149-2150 2151-2152 2153-2154 2155-2156 2157-2158 2159-2160 2161-2162 2163-2164 2165-2166 2167-2168 2169-2170 2171-2172 2173-2174 2175-2176 2177-2178 2179-2180 2181-2182 2183-2184 2185-2186 2187-2188 2189-2190 2191-2192 2193-2194 2195-2196 2197-2198 2199-2200 2201-2202 2203-2204 2205-2206 2207-2208 2209-2210 2211-2212 2213-2214 2215-2216 2217-2218 2219-2220 2221-2222 2223-2224 2225-2226 2227-2228 2229-2230 2231-2232 2233-2234 2235-2236 2237-2238 2239-2240 2241-2242 2243-2244 2245-2246 2247-2248 2249-2250 2251-2252 2253-2254 2255-2256 2257-2258 2259-2260 2261-2262 2263-2264 2265-2266 2267-2268 2269-2270 2271-2272 2273-2274 2275-2276 2277-2278 2279-2280 2281-2282 2283-2284 2285-2286 2287-2288 2289-2290 2291-2292 2293-2294 2295-2296 2297-2298 2299-2300 2301-2302 2303-2304 2305-2306 2307-2308 2309-2310 2311-2312 2313-2314 2315-2316 2317-2318 2319-2320 2321-2322 2323-2324 2325-2326 2327-2328 2329-2330 2331-2332 2333-2334 2335-2336 2337-2338 2339-2340 2341-2342 2343-2344 2345-2346 2347-2348 2349-2350 2351-2352 2353-2354 2355-2356 2357-2358 2359-2360 2361-2362 2363-2364 2365-2366 2367-2368 2369-2370 2371-2372 2373-2374 2375-2376 2377-2378 2379-2380 2381-2382 2383-2384 2385-2386 2387-2388 2389-2390 2391-2392 2393-2394 2395-2396 2397-2398 2399-2400 2401-2402 2403-2404 2405-2406 2407-2408 2409-2410 2411-2412 2413-2414 2415-2416 2417-2418 2419-2420 2421-2422 2423-2424 2425-2426 2427-2428 2429-2430 2431-2432 2433-2434 2435-2436 2437-2438 2439-2440 2441-2442 2443-2444 2445-2446 2447-2448 2449-2450 2451-2452 2453-2454 2455-2456 2457-2458 2459-2460 2461-2462 2463-2464 2465-2466 2467-2468 2469-2470 2471-2472 2473-2474 2475-2476 2477-2478 2479-2480 2481-2482 2483-2484 2485-2486 2487-2488 2489-2490 2491-2492 2493-2494 2495-2496 2497-2498 2499-2500 2501-2502 2503-2504 2505-2506 2507-2508 2509-2510 2511-2512 2513-2514 2515-2516 2517-2518 2519-2520 2521-2522 2523-2524 2525-2526 2527-2528 2529-2530 2531-2532 2533-2534 2535-2536 2537-2538 2539-2540 2541-2542 2543-2544 2545-2546 2547-2548 2549-2550 2551-2552 2553-2554 2555-2556 2557-2558 2559-2560 2561-2562 2563-2564 2565-2566 2567-2568 2569-2570 2571-2572 2573-2574 2575-2576 2577-2578 2579-2580 2581-2582 2583-2584 2585-2586 2587-2588 2589-2590 2591-2592 2593-2594 2595-2596 2597-2598 2599-2600 2601-2602 2603-2604 2605-2606 2607-2608 2609-2610 2611-2612 2613-2614 2615-2616 2617-2618 2619-2620 2621-2622 2623-2624 2625-2626 2627-2628 2629-2630 2631-2632 2633-2634 2635-2636 2637-2638 2639-2640 2641-2642 2643-2644 2645-2646 2647-2648 2649-2650 2651-2652 2653-2654 2655-2656 2657-2658 2659-2660 2661-2662 2663-2664 2665-2666 2667-2668 2669-2670 2671-2672 2673-2674 2675-2676 2677-2678 2679-2680 2681-2682 2683-2684 2685-2686 2687-2688 2689-2690 2691-2692 2693-2694 2695-2696 2697-2698 2699-2700 2701-2702 2703-2704 2705-2706 2707-2708 2709-2710 2711-2712 2713-2714 2715-2716 2717-2718 2719-2720 2721-2722 2723-2724 2725-2726 2727-2728 2729-2730 2731-2732 2733-2734 2735-2736 2737-2738 2739-2740 2741-2742 2743-2744 2745-2746 2747-2748 2749-2750 2751-2752 2753-2754 2755-2756 2757-2758 2

1. The first part of the document is a letter from the President of the United States to the Congress, dated January 1, 1861. It is a very important document, as it sets out the President's policy for the new year. The President states that he will continue to support the Union, and will use all the powers of the Executive to maintain the peace and harmony of the country. He also mentions the recent events in the South, and expresses his concern for the future of the Union.

... ..
... ..
... ..

— 10 —

1. The first step is to identify the problem or goal. This involves understanding the current situation and what needs to be achieved.

ALL INFORMATION CONTAINED HEREIN IS UNCLASSIFIED
DATE 08-01-2001 BY 60322 UCBAW

1. The first group of people who are likely to be affected by the proposed project are the local residents who live in the vicinity of the project site. These residents may be affected by the project in a number of ways, including increased traffic, noise, and air pollution. It is important to identify these potential impacts and to develop measures to mitigate them.

[illegible]

1. The first part of the report is a general introduction to the project, which includes a brief history of the organization and a statement of its mission.

APPENDIX A

THE VOLTAGE COUPLING COEFFICIENTS FOR THE TE₁₀ MODE AS DEVELOPED FROM BETHE'S SMALL HOLE THEORY

Bethe¹ describes the voltage coupled through a small aperture by three lumped constants, namely two magnetic polarizabilities, M_1 and M_2 , and one electric polarizability, P . These constants determine the effect of any aperture on the wave guide. For simple shapes such as circles, ellipses, and slits, these polarizabilities have been calculated. Note that these constants are independent of the field. They depend only on the geometry of the aperture.

For the TE₁₀ mode, Bethe's formula for the voltage coefficient for the forward wave is

$$A = \frac{j\pi}{\lambda_0 S} (P E_{y1} E_{y2} - M_1 H_{x1} H_{x2} - M_2 H_{z1} H_{z2}) e^{-j(\omega t - \beta z)} \quad (46)$$

where λ_0 = free space wave-length

S = normalizing factor $\frac{2a^3 bc^2}{\lambda_g \lambda_0}$

P = electric polarizability for a round hole = $2r^3/3$

M_1 = transverse magnetic polarizability for a round hole = $4r^3/3$

M_2 = longitudinal magnetic polarizability for a round hole = $4r^3/3$

E_{y1}, H_{x1}, H_{z1} - field components in the main guide

E_{y2}, H_{x2}, H_{z2} = field components in the auxiliary guide

$$\beta = \frac{2\pi}{\lambda_g} \quad \lambda_g \text{ is guide wave length}$$

x is the principal axis in the direction of the large guide dimension, a

y is the principal axis in the direction of the small guide dimension, b

z is the principal axis in the longitudinal direction

The component fields for the TE_{10} Mode are

$$H_z = C \cos \pi x / a$$

$$H_x = \frac{j2aC}{\lambda_g} \sin \pi x / a$$

$$E_y = \frac{-j2aC}{\lambda_0} \sin \pi x / a \quad \text{where } C \text{ is a constant.}$$

For small holes $E_{y1} = E_{y2}$; $H_{x1} = H_{x2}$; and $H_{z1} = H_{z2}$.

Omitting for the time being the exponential factor and substituting the above equations into equation (46).

$$A = \frac{j2\pi r^3}{3a^2b} \left(\frac{\lambda_g}{2a} \right)^2 \left[\left(\frac{2a}{\lambda_0} \right)^2 \sin^2 \frac{\pi x}{a} - 2 \left(\frac{2a}{\lambda_g} \right) \sin^2 \frac{\pi x}{a} - 2 \left(\cos^2 \frac{\pi x}{a} \right) \right] \quad (47)$$

factoring our $2a/\lambda_g$ gives

$$A = \frac{j2\pi r^3}{3a^2b} \left[\left(\frac{2a}{\lambda_0} \right)^2 \left(\frac{\lambda_g}{2a} \right) \sin^2 \frac{\pi x}{a} - 2 \left(\frac{2a}{\lambda_g} \right) \sin^2 \frac{\pi x}{a} - 2 \left(\frac{\lambda_g}{2a} \right) \cos^2 \frac{\pi x}{a} \right] \quad (48)$$

Now making use of the identity, $\frac{1}{\lambda_0^2} = \frac{1}{4a^2} + \frac{1}{\lambda_g^2}$, λ_0 may be eliminated from the equation (48), leaving

$$A = \frac{j2\pi r^3}{3a^2b} \left[\left(\frac{\lambda_g}{2a} + \frac{2a}{\lambda_g} \right) \sin^2 \frac{\pi x}{a} - \left(\frac{2a}{\lambda_g} \right) 2 \sin^2 \frac{\pi x}{a} - \left(\frac{\lambda_g}{2a} \right) 2 \cos^2 \frac{\pi x}{a} \right] \quad (49)$$

For the case of $\lambda = 0$, the equation becomes

$$x^2 - 1 = 0$$

which has the roots $x = 1$ and $x = -1$.

For the case of $\lambda \neq 0$, the equation becomes

$$x^2 - \lambda x + 1 = 0$$

which has the roots $x = \frac{\lambda \pm \sqrt{\lambda^2 - 4}}{2}$.

$$x = \frac{\lambda + \sqrt{\lambda^2 - 4}}{2}$$

$$x = \frac{\lambda - \sqrt{\lambda^2 - 4}}{2}$$

$$x = \frac{\lambda \pm \sqrt{\lambda^2 - 4}}{2}$$

For small values of λ , the roots are approximately

obtained by expanding the square root in a power series.

Substituting the above expression for the roots into the equation

$$x^2 - \lambda x + 1 = 0$$

gives the following result:

$$x = \frac{\lambda \pm \sqrt{\lambda^2 - 4}}{2}$$

Now, using the binomial expansion, we can write the square root as

$$\sqrt{\lambda^2 - 4} = 2 \sqrt{1 - \frac{\lambda^2}{4}}$$

This is the equation for determining the forward coupled voltage in a common guide wall of zero thickness. If this wall has a finite thickness, the electric term will have an attenuation coefficient, α_E , and the magnetic terms have an attenuation coefficient, α_H . This results in the following final equation which is used in the text:

$$A = j \frac{2\pi r^3}{3a^2b} \left[\alpha_E \left(\frac{\lambda_g}{2a} + \frac{2a}{\lambda_g} \right) \sin^2 \frac{\pi x}{a} - 2\alpha_H \left(\frac{2a}{\lambda_g} \right) \sin^2 \frac{\pi x}{a} - 2\alpha_H \left(\frac{\lambda_g}{2a} \right) \cos^2 \frac{\pi x}{a} \right] \quad (50)$$

with

$$\begin{aligned} \alpha_E &= f(t, \lambda) \\ \alpha_H &= f(t, \lambda) \end{aligned} \quad t \text{ is thickness}$$

The voltage coefficient due to the backward wave is developed in an identical manner, differing only in signs as indicated below.

$$B = j \frac{2\pi r^3}{3a^2b} \left[\alpha_E \left(\frac{\lambda_g}{2a} + \frac{2a}{\lambda_g} \right) \sin^2 \frac{\pi x}{a} + 2\alpha_H \left(\frac{2a}{\lambda_g} \right) \sin^2 \frac{\pi x}{a} - 2\alpha_H \left(\frac{\lambda_g}{2a} \right) \cos^2 \frac{\pi x}{a} \right] \quad (51)$$

This is the same as the statement of the
a son in the same way. The same is the
statement, the statement of the same is the
statement, and the statement of the same is the
statement. This results in the following statement.

Text:

with
The voice of the same is the same as the
in an identical manner, the same is the
statement.

APPENDIX B

THE DEVELOPMENT OF THE HOLE DIAMETERS FOR FORWARD VOLTAGE COUPLING COEFFICIENTS PROPORTIONAL TO TCHEBYSCHIEFF POLYNOMIAL COEFFICIENTS

Dolph's method of computing the Tchebyscheff coefficients for an antenna with $2N$ elements can be applied to a directional coupler with $2N$ apertures or holes. These coefficients will be made proportional to the forward voltage coupling coefficients rather than the feed currents of an antenna array.

Selecting $2N$ as ten gives

$$F_{2N}(\theta) = \sum_{n=1}^N t'_n \cos(2n-1)\theta \quad (52)$$

$$= t'_1 \cos \theta + t'_2 \cos 3\theta + t'_3 \cos 5\theta + t'_4 \cos 7\theta + t'_5 \cos 9\theta$$

The non-normalized Tchebyscheff polynomials for $\cos(2n-1)\theta$ are for

$$n=1, \cos \theta = x$$

$$2, \cos 3\theta = 4x^3 - 3x$$

$$3, \cos 5\theta = 16x^5 - 20x^3 + 5x$$

$$4, \cos 7\theta = 64x^7 - 112x^5 + 56x^3 - 7x$$

$$5, \cos 9\theta = 256x^9 - 576x^7 + 432x^5 - 120x^3 + 9x$$

Substituting these in (52) above

$$G_{2N-1}(x) = t'_1 x + t'_2 (3x - 4x^3) + t'_3 (5x - 20x^3 + 16x^5) + t'_4 (7x - 56x^3 + 112x^5 - 64x^7) + t'_5 (9x - 120x^3 + 432x^5 - 576x^7 + 256x^9) \quad (53)$$

and then regrouping the terms gives

$$G_{2N-1}(x) = 256 t'_5 x^9 + (-576 t'_5 + 64 t'_4) x^7 + (432 t'_5 - 112 t'_4 + 16 t'_3) x^5 + (-120 t'_5 + 56 t'_4 - 20 t'_3 + 4 t'_2) x^3 + (9 t'_5 - 7 t'_4 + 5 t'_3 + 3 t'_2 + t'_1) x \quad (54)$$

The Tchebyscheff polynomial of order $2N-1$ or 9, in z_0x is

$$T_9(z_0x) = 256x^9z_0^9 - 576x^7z_0^7 + 432x^5z_0^5 - 120x^3z_0^3 + 9xz_0 \quad (55)$$

Equating equations (54) and (55) by setting like coefficients of x equal gives

$$t'_5 = z_0^9 \quad (56)$$

$$t'_4 = 9(t'_5 - z_0^7) \quad (57)$$

$$t'_3 = -27(t'_5 - z_0^5) + 7t'_4 \quad (58)$$

$$t'_2 = 30(t'_5 - z_0^3) - 14t'_4 + 5t'_3 \quad (59)$$

$$t'_1 = -9(t'_5 - z_0) + 7t'_4 - 5t'_3 + 3t'_2 \quad (60)$$

The parameter, z_0 , may be solved for by the following formula:

$$z_0 = \frac{1}{2} \left[(g + \sqrt{g^2 - 1})^{1/m} + (g - \sqrt{g^2 - 1})^{1/m} \right]$$

For g equal to 1500 and m equal to 9,

$$z_0 \approx \frac{1}{2} \left[(2g)^{1/m} + (1/2g)^{1/m} \right] = 1.422$$

Substituting this value of z_0 in equations (56) through (60), the non-normalized Tchebyscheff coefficients are obtained.

$$t'_5 = 20.60$$

$$t'_4 = 91.05$$

$$t'_3 = 225.16$$

$$t'_2 = 387.69$$

$$t'_1 = 501.51$$

1. The first of these is the fact that the

the first of these is the fact that the

the first of these is the fact that the

(1)

(2)

(3)

(4)

The first of these is the fact that the

the first of these is the fact that the

the first of these is the fact that the

the first of these is the fact that the

From these, the normalized coefficients are

$$\begin{aligned}t_5 &= 1.00 \\t_4 &= 4.42 \\t_3 &= 10.93 \\t_2 &= 18.82 \\t_1 &= 24.35\end{aligned}$$

These coefficients must now be placed equal to the forward coupling coefficients, A_n , where n goes from 1 to 10, corresponding to the holes of the ten coupling elements. t_5 was made proportional to A_1 and A_{10} because of symmetry. $t_4 \propto A_2$ and A_9
 $t_3 \propto A_3$ and A_8
 $t_2 \propto A_4$ and A_7
 $t_1 \propto A_5$ and A_6

For a -3 db coupler the holes corresponding to these coupling coefficients would be too large to conform with Bethe's small hole theory. Four ten element arrays with the voltage coefficients superimposed as shown in figure (7), were used.

Array #1	$t_5 t_4 t_3 t_2 t_1 t_1 t_2 t_3 t_4 t_5$	
Array #2	$t_5 t_4 t_3 t_2 t_1 t_1 t_2 t_3 t_4 t_5$	
Array #3	$t_5 t_4 t_3 t_2 t_1 t_1 t_2 t_3 t_4 t_5$	
Array #4	$t_5 t_4 t_3 t_2 t_1 t_1 t_2 t_3 t_4 t_5$	
Element	1 2 3 4 5 6 7 8 9 10 11 12 13 14 15 16 17 18 19 20 21 22	
	Line of Symmetry	

The value of the final T_n coefficients (where n is the total number of elements and now goes from 1 to 22) for a given element is the sum of the vertical column above the particular element to be computed.

From these, the following results were obtained:

[illegible]

These coefficients must be a function of the coupling coefficient, k , and the coupling coefficient, k , must be a function of the coupling coefficient, k .

For a -3 Is implies the polar coordinates are given by
coefficient would be too large to compute the 300% will take
theory. Your can't have it all at once. The 300% will take
imposed as shown in Figure (7), were used.

[illegible]

[Faint handwritten text]

44-38861-1000

[Faint handwritten notes at the bottom of the page]

TELETYPE UNIT 1 9 7 0 4 5 2 1 memo 18
 10/10/70 10:00

The value of each column is calculated by multiplying the number of elements in the row by the value of the element in the column. The sum of the values of all columns is the total value of the matrix.

Due to symmetry the following tabulation need be made only for eleven elements:

T_1	T_2	T_3	T_4	T_5	T_6	T_7	T_8	T_9	T_{10}	T_{11}
1.00	4.42	10.93	18.82	24.35	24.35	18.82	10.93	4.42	1.00	
				1.00	4.42	10.93	18.82	24.35	24.35	18.82
								1.00	4.42	10.93

1.00 4.42 10.93 18.82 25.35 28.77 29.75 29.75 29.77 29.77 29.75

The total sum of the 22 Tchebyscheff coefficients as modified by the superimposition is

$$T_T = 2 \sum_{n=1}^{11} T_n = 476.16$$

For coupling of -3 db,

$$-3 \text{ db} = 20 \log A_T ; \text{ then } A_T = 0.708$$

where A_T is the total of the voltage coefficients to be coupled.

Then by the simple relation $2xT_T/T_n = A_T/A_n$, the voltage coefficient for hole n , A_n , was computed. The two in this relation is for the two rows of 22 elements.

The transcendental equation for A_n was plotted by assuming values of r_n . Then by computing the values of A_n from this equation, the radii of the 11 different sized coupling holes was obtained from this plot. For accuracy, the value of the radii obtained from the plot was substituted in the equation for A_n to check if the correct value of voltage was coupled.

TABULATION of A_n AND D_n

$A_1(A_{22}) = 7.426 \times 10^{-4}$	$d_1 = .121''$
$A_2(A_{21}) = 3.282 \times 10^{-3}$	$d_2 = .184$
$A_3(A_{20}) = 8.117 \times 10^{-3}$	$d_3 = .240$
$A_4(A_{19}) = 1.398 \times 10^{-2}$	$d_4 = .282$
$A_5(A_{18}) = 1.982 \times 10^{-2}$	$d_5 = .308$
$A_6(A_{17}) = 2.136 \times 10^{-2}$	$d_6 = .320$
$A_7(A_{16}) = 2.209 \times 10^{-2}$	$d_7 = .324$
$A_8(A_{15}) = 2.209 \times 10^{-2}$	$d_8 = .324$
$A_9(A_{14}) = 2.211 \times 10^{-2}$	$d_9 = .324$
$A_{10}(A_{13}) = 2.211 \times 10^{-2}$	$d_{10} = .324$
$A_{11}(A_{12}) = 2.209 \times 10^{-2}$	$d_{11} = .324$

IT CAN BE TO THE POINT

1. 1. 1	1. 1. 1
2. 1. 1	2. 1. 1
3. 1. 1	3. 1. 1
4. 1. 1	4. 1. 1
5. 1. 1	5. 1. 1
6. 1. 1	6. 1. 1
7. 1. 1	7. 1. 1
8. 1. 1	8. 1. 1
9. 1. 1	9. 1. 1
10. 1. 1	10. 1. 1
11. 1. 1	11. 1. 1
12. 1. 1	12. 1. 1
13. 1. 1	13. 1. 1
14. 1. 1	14. 1. 1
15. 1. 1	15. 1. 1
16. 1. 1	16. 1. 1
17. 1. 1	17. 1. 1
18. 1. 1	18. 1. 1
19. 1. 1	19. 1. 1
20. 1. 1	20. 1. 1



JUL 2
FEB 8
MAY 11
4 MAY 71

BINDERY
889
RENEWED
DISPLAY
18600

Thesis

E27

Eidson

20753

A broad band bi-directional
coupler with tight coupling
and high directivity

★
FEB 8
MAR 11
MAY 11
4 MAY 71

BINDERY
889
RENEWED
DISPLAY
18600

Thesis

E27

Eidson

20753

A broad band bi-directional coupler
with tight coupling and high directi-
vity

Library
U. S. Naval Postgraduate School
Monterey, California



thesE27

A broad band bi-directional coupler with



3 2768 001 90374 3

DUDLEY KNOX LIBRARY